DTIC FILE COPY

AFRPL TR-86-096 AD:

AD-A179 814

Final Report
for the period
1 August 1983 to
1 September 1986

Propellant Aging Research

DTIC
ELECTE
APR 3 0 1987
S D
D

February 1987

Authors:
D. B. Olson
R. J. Gill

AeroChem Research Laboratories, Inc.
P. O. Box 12
Princeton, NJ 08542

TP-460
F04611-83-C-0037

Approved for Public Release

Distribution is unlimited. The AFRPL Technical Services Office has reviewed this report, and it is releaseable to the National Technical Information Service, where it will be available to the general public, including foreign nationals.

prepared for the: **Air Force Rocket Propulsion Laboratory**

Air Force Space Technology Center
Space Division, Air Force Systems Command
Edwards Air Force Base,
California 93523-5000

87 4 29 044

NOTICE

When U.S. Government drawings, specifications, or other data are used for any purpose other than a definitely related Government procurement operation, the fact that the Government may have formulated, furnished, or in any way supplied the said drawings, specifications, or other data, is not to be regarded by implication or otherwise, or in any way licensing the holder or any other person or corporation, or conveying any rights or permission to manufacture, use, or sell any patented invention that may be related thereto.

FOREWORD

This report describes the work accomplished by AeroChem Research Laboratories, Inc. under contract F04611-83-C-0037 with the Air Force Rocket Propulsion Laboratory (AFRPL), Edwards Air Force Base, California. AFRPL Project Manager was Berge Goshgarian.

This report has been reviewed and is approved for release and distribution in accordance with the distribution statement on the cover and on the DD Form 1473.

BERGE G. GOSHGARIAN
Project Manager

FRANCISCO Q. ROBERTO
Chief, Propellant Development Branch

FOR THE COMMANDER

KENNETH E. MURPHY, Lt Col, USAF
Deputy Director
Solid Rocket Division

UNCLASSIFIED

SECURITY CLASSIFICATION OF THIS PAGE

REPORT DOCUMENTATION PAGE

1a. REPORT SECURITY CLASSIFICATION UNCLASSIFIED	1b. RESTRICTIVE MARKINGS
2a. SECURITY CLASSIFICATION AUTHORITY	3. DISTRIBUTION/AVAILABILITY OF REPORT APPROVED FOR PUBLIC RELEASE. Distribution is Unlimited.
2b. DECLASSIFICATION/DOWNGRADING SCHEDULE	
4. PERFORMING ORGANIZATION REPORT NUMBER(S) TP-460	5. MONITORING ORGANIZATION REPORT NUMBER(S) AFRPL-TR-86-096
6a. NAME OF PERFORMING ORGANIZATION AeroChem Research Laboratories, Inc. 6b. OFFICE SYMBOL (If applicable)	7a. NAME OF MONITORING ORGANIZATION Air Force Rocket Propulsion Laboratory
6c. ADDRESS (City, State and ZIP Code) P.O. Box 12 Princeton, New Jersey 08542	7b. ADDRESS (City, State and ZIP Code) MKPB Edwards Air Force Base, CA 93523-5000
8a. NAME OF FUNDING/SPONSORING ORGANIZATION 8b. OFFICE SYMBOL (If applicable)	9. PROCUREMENT INSTRUMENT IDENTIFICATION NUMBER F04611-83-C-0037
8c. ADDRESS (City, State and ZIP Code)	10. SOURCE OF FUNDING NOS PROGRAM ELEMENT NO. 61102F; PROJECT NO. 2302; TASK NO. M1; WORK UNIT NO. AC
11. TITLE (Include Security Classification) Propellant Aging Research (U)	
12. PERSONAL AUTHOR(S) Olson, Douglas B. and Gill, Robert J.	
13a. TYPE OF REPORT Final 13b. TIME COVERED FROM 83-8-1 TO 86-9-1	14. DATE OF REPORT (Yr., Mo., Day) 87/2 15. PAGE COUNT 77
16. SUPPLEMENTARY NOTATION Keywords:	
17. COSATI CODES FIELD 21, GROUP 09 FIELD 17, GROUP 03 SUB. GR.	18. SUBJECT TERMS (Continue on reverse if necessary and identify by block number) Propellant aging; Energetic materials; ~~Thermal decomposition~~; Kinetics; ~~Chemiluminescence~~

19. ABSTRACT (Continue on reverse if necessary and identify by block number)

Chemical aging of solid rocket propellants and ingredients was studied. The thermal decomposition rate coefficients of cyclotrimethylene trinitramine, butanetriol trinitrate, and ammonium perchlorate were measured from about 310 to 375 K using a NO_x^- chemiluminescence analyzer. The decomposition of butanetriol trinitrate was shown to undergo a mechanism change at 333 K. Six cured mixtures of hydroxy terminated polybutadiene binder, ammonium perchlorate, aluminum, and stabilizer were prepared, exposed to four reactive gases for 54 hours at 344 K, and analyzed for weight change, sol/gel content, and molecular weight of sol. These techniques were not sensitive enough to reliably analyze early changes due to chemical aging. Polymer chemiluminescence resulting from chemical degradation of this series of propellant mixtures by reactive gases was also studied from 300 to 350 K. This work showed that the stabilizer methylnitroaniline significantly reduces chemical reactions occurring upon exposure to air but not upon exposure to NO_2/air. The

20. DISTRIBUTION/AVAILABILITY OF ABSTRACT UNCLASSIFIED/UNLIMITED ☒ SAME AS RPT. ☐ OTIC USERS ☐	21. ABSTRACT SECURITY CLASSIFICATION Unclassified
22a. NAME OF RESPONSIBLE INDIVIDUAL Berge G. Goshgarian	22b. TELEPHONE NUMBER (Include Area Code) (805) 275-5209 22c. OFFICE SYMBOL MKPB

DD FORM 1473, 83 APR EDITION OF 1 JAN 73 IS OBSOLETE.

UNCLASSIFIED

SECURITY CLASSIFICATION OF THIS PAGE

Block 19 (continued)

results of this program demonstrate the capabilities of the real-time NO_x offgas analysis technique and the polymer chemiluminescence technique.

FLD 18

QUALITY INSPECTED 1

Accesion For
NTIS CRA&I
DTIC TAB
Unannounced
Justification
By
Distribution /
Availability Codes
Dist | Avail and / or Special
A-1

TABLE OF CONTENTS

LIST OF TABLES

LIST OF FIGURES

1. INTRODUCTION

Solid rocket propellants undergo slow physical and chemical changes over their long (sometimes greater than ten year) service lifetimes. The specific type of changes depends on the composition of the propellant formulation, but in general there are small chemical changes which alter the mechanical properties of the propellant. Some propellants harden with age whereas others soften; in either case the operation of the rocket motor is threatened. Many current propellants use hydroxy-terminated polybutadiene, HTPB, as the polymer binder which holds together the propellant ingredients, a majority of which may be solids. A typical composite propellant might be 15% HTPB, curing agent and minor ingredients, such as an antioxidant, combined with 85% of a mixture of ammonium perchlorate, AP, and aluminum, Al. These propellants harden with age and may ultimately crack. A rocket motor with a cracked propellant grain will probably fail in use, causing the loss of the mission or payload and it may endanger personnel. Thus, aging of propellants is of great concern to the Air Force.

The objective of this project was to gain an improved understanding of the chemical processes and rate parameters responsible for chemical aging of solid rocket propellants. The working hypothesis was that aging occurs as a result of attack on polymer binders and stabilizers by products released in the slow decomposition of the oxidizers and/or plasticizers. It was assumed that the degradation of the binders causes the most serious changes in the propellant mechanical properties. The initial part of this work involved measuring the thermal decomposition rate coefficients of several important energetic materials from near room temperature up to about 400 K. The materials chosen for study were the nitramine hexahydro-1,3,5-trinitro-s-triazine (more commonly known as RDX or cyclotrimethylene trinitramine), ammonium perchlorate, and a highly energetic liquid nitrate ester plasticizer, butanetriol trinitrate, BTTN. The decomposition of these materials was studied using a previously developed highly sensitive offgas analysis technique, in which a slow flow of inert gas is passed over samples held at constant temperature; the small quantity of offgas NO_x or NH_3 produced by the decomposition reactions is measured. The decomposition rate coefficient was therefore determined from the measurement of the number of moles of NO_x produced per second

per mole of the material. Under our conditions of very small concentrations of gaseous decomposition products and brief exposure to the starting material, few secondary reactions were expected other than reduction of NO_2 to NO. A specialized chemiluminescence NO_x analyzer, based on the measurement of light emission from the reaction of ozone with NO, was used to measure these small concentrations. Our apparatus is capable of measuring less than 1 part NO_x in 10^9 parts of nitrogen in real time and using small carrier gas flows.

The second objective of the program was to study the kinetics of the reactions of various HTPB-containing mixtures with gases which may be produced from the slow decomposition of propellant components. These data provide the basis for developing more accurate models of the aging chemistry of HTPB binder. The reactions of gaseous decomposition products with binder were probed in several experiments. A series of propellant mixtures was exposed to different gases under mild aging conditions and then analyzed for the resulting changes by weight loss or gain, sol/gel content measurements, and liquid chromatographic analysis of the molecular weight distribution of the sol content of HTPB. In separate experiments this series of propellant mixtures was exposed to reactive gases and the intensity of chemiluminescence from the binder reactions measured. This technique of using the polymer chemiluminescence, CL, as a measurement of the reaction rate has been employed previously to study oxidation reactions of both polymers and liquid hydrocarbons (Ref. 1) and is a very sensitive technique. In a previous AFRPL-funded program (Ref. 2) at SRI International, Davenport and Mayo applied polymer CL to measurements on HTPB propellant aging. The main differences between their work and this program were that SRI attempted to correlate the CL from propellant samples with how long they had been aged (up to 78 weeks), and they performed most of their CL measurements at higher temperatures and in different gas environments (N_2 and air) than we used. None of our samples were aged; they were cured at 327 K (54°C) for 10 days and then stored at about 278 K in a nitrogen filled desiccator. Our experiments were designed to measure the reactivity of the binder and binder mixtures with reagent gases. This might be called a measurement of an aging rate. The SRI experiments were designed to measure the change in CL in air or N_2 as a function of age (possibly resulting from the buildup of reaction products with long times, depletion of some ingredient, or maybe as the result of changes in the binder network). The apparatuses were similar.

2. SUMMARY

The objective of this project was to gain an improved understanding of the chemical processes and rate parameters responsible for chemical aging of solid rocket propellants. The working hypothesis was that aging occurs as a result of attack on polymer binders and stabilizers by products released in the slow decomposition of the oxidizers and/or plasticizers. The program consisted of two types of study; measurements of the thermal decomposition rate coefficients of three important energetic materials, RDX, AP, and BTTN and measurements of the reactivity of a series of increasingly complex HTPB-containing propellant mixtures. These latter tests were performed using measurements of the weight change, sol/gel fractions, molecular weight distribution of the sol, and polymer chemiluminescence from samples exposed to reactive gases.

The thermal decomposition rate coefficients of RDX, AP, and BTTN were measured by determining the rate of NO_x evolution (NH_3 from AP) from small samples as a function of temperature from about 310 to 373 K (37 to 100°C). The data points were fitted using weighted nonlinear least squares routines to yield the following rate coefficient expressions:

$$k(RDX) = 10^{4.9 \pm 0.5} \exp[-(12,430 \pm 700)/T] \quad s^{-1} \quad 316 \text{ to } 376 \text{ K } (43 \text{ to } 103°C)$$

$$k(AP) = 10^{7.6 \pm 1.5} \exp[-(14,950 \pm 1,260)/T] \quad s^{-1} \quad 343 \text{ to } 383 \text{ K } (70 \text{ to } 110°C)$$

$$k(BTTN) = 10^{19.1 \pm 2.0} \exp[-(22,400 \pm 1,660)/T] + 10^{1.8 \pm 2.9} \exp[-(9,060 \pm 2,100)/T] \quad s^{-1} \quad 309 \text{ to } 360 \text{ K } (36 \text{ to } 87°C)$$

These data are unique; no previous real time measurements of these rate coefficients exist in these temperature ranges. The results for RDX yield a small activation energy, 103 kJ/mol, compared to the value obtained (Ref.3), 203 kJ/mol, for the liquid RDX decomposition at about 483 K (210°C) and to the gas phase activation energy for $N\text{-}NO_2$ bond cleavage in other molecules. Yet, in comparison with work previously done where both gas phase and solid phase decompositions occur simultaneously, the value obtained in this work, extrapolated to higher temperatures, supports the observation and conclusion from that work.

The result for AP decomposition is in approximate agreement with earlier work performed at higher temperatures where the rate coefficient is four to six decades larger. However, the variety of rate coefficients obtained at

higher temperatures exhibits a range of activation energies such that any extrapolation down to room temperature has a one to two decade uncertainty. The current results extend down to 343 K and allow a much more precise value to be calculated for lower temperatures.

Highly energetic nitrate esters, including nitroglycerin, NG, used to plasticize propellants are considerably less stable than most other ingredients, making them the limiting factor in the service lifetime of many of these propellants. Stabilizers to react with the NO_x generated by nitrate ester decomposition must be included in the propellant formulations. In addition, the concentration of the nitrate ester is sometimes reduced due to its evaporation and migration through the propellant, but this can be mostly overcome by sealing the motor. Our measurements of the rate coefficient for BTTN decomposition were complicated by the decomposition in the thermal converter of the small amount of BTTN vapor picked up in the carrier gas flow, and thus detected as "false" NO_x. A cold trap installed in the line between the samples and analyzer to selectively remove BTTN vapor but not NO or NO_2 made rate determinations possible. The results of these measurements using the vapor trap show that the rate coefficient for BTTN decomposition undergoes a change in slope at a temperature of about 333 K (60°C), indicating that a change in the BTTN decomposition mechanism probably occurs at this temperature. Above 333 K the decomposition process is dominated by a higher activation energy, 184 kJ/mol, process, whereas below 333 K a process with a much lower activation energy, 75 kJ/mol, dominates. This behavior, previously observed, Ref. 4, for nitrocellulose decomposition, is extremely important for estimating the rate of NO_x generation of aging propellants containing nitrate esters. Extrapolating rate coefficient data obtained in the temperature regime above this transition leads to estimates of low temperature stability far in excess of actual. Thus service lifetimes estimated using high temperature rate coefficient data and activation energies might be 10 to 50 times too long. This emphasizes the need for kinetic studies to be performed over broad temperature ranges (to accurately determine activation energies) and close to the actual temperatures of interest. For most propellant stability work, this leads to the need for highly sensitive techniques for measuring small concentrations of offgas species and small rate coefficients. The AeroChem chemiluminescence

NO_x analysis technique can measure rate coefficients as small as 10^{-13} s^{-1}, under conditions where little or no secondary reactions occur.

The two-process decomposition of BTTN found in this work and observed previously for NC strongly suggests the general conclusion that other nitrate esters with two or more O-NO_2 groups located in different molecular environments (i.e., with different closest neighbors and proximity to other O-NO_2 groups) will exhibit similar-two process decomposition. This may include NG, and in fact Layton and coworkers, Ref. 5, measuring propellant aging rates using CO_2 offgas concentrations, found a change in temperature dependence from 172 to 26 kJ/mol at about 333 K (60°C) for a NG containing propellant.

Binder reactivity measurements were performed on a series of HTPB containing mixtures with and without the following ingredients: TPB cure catalyst; MNA stabilizer; AP; and Al. Samples of these mixtures were exposed to N_2, air, NO, and a mixture of 5.5% NO_2/94.5% air for 54 h at 344 K (71°C). These aging conditions were considered to be mild, yet in many cases the sample discs were visibly altered by the tests. Many samples hardened and changed color. The simplest measurement, that of weight change after exposure, showed the least weight gain for exposure under N_2 and also demonstrated the effectiveness of the MNA stabilizer in preventing oxidation of the binder by air. However, this stabilizer appears to be much less effective for propellants exposed to NO or NO_2/air. The samples with solids added (AP or AP and Al) showed no significantly greater weight gains than the samples without the solids.

The main observations from the sol/gel analyses were that the TPB cure catalyst noticeably decreases the sol fraction (as expected by enhancing the polymerization) and that the samples with added solids give significantly larger sol fractions. Surprisingly, no real differences in sol fraction were found among samples exposed to the different reactive gas environments. The GPC analyses of the polymer molecular weight distributions in these sol fractions also showed only minor differences. The complete number and weight

distributions are given below for each sample exposed to each gas environment.* Exposure to NO yielded a slightly larger MW for most samples. No significant differences were seen between the samples with and without solids as was the case in the sol fraction data. This indicates that AP addition, and even more so, AP and Al addition, greatly increases the sol weight fraction without changing the MW of the polymer in the sol. This probably means that the cure reactions were hindered by the solids. There is no evidence that the exposure to reactive gases was necessary for this difference to exist. In general, however, the results obtained in this work indicate that sol/gel fraction analysis and molecular weight analysis by GPC are not sufficiently sensitive, or are not sensitive to the right factors, to easily and reliably show very small changes in this type of propellant. Our results indicate that more sensitive or reliable techniques are needed.

The polymer chemiluminescence, CL, measurements of propellant reactions were performed with a relatively simple apparatus, consisting of a heated sample stage contained in a gas and light tight housing and having a thermally insulated window to a photomultiplier detector. Since the observed light levels are low, photon counting electronics were used; light intensities of less than one photon per second greater than background were measurable. It was found that consistency in sample curing and handling procedures was necessary. Difficulties were initially encountered in the reproducibility of the chemiluminescence data. We think that additional cure reactions were occurring during these CL measurement experiments in which the samples were heated to 353 K (80°C), and that these reactions then altered the sample CL when the lower temperature measurements were repeated. Good consistency and repeatability of the CL data were obtained by giving all samples a 24 h exposure to N_2 with the samples at 359 K prior to CL experiments.

All of the CL data exhibited Arrhenius behavior, that is, yielded a straight line when the logarithm of the CL intensity (photon count rate) was plotted vs. inverse temperature. In each case, the data obtained from samples exposed to N_2 and to NO were similar and were about a factor of 15 smaller than the data obtained from samples exposed to air or NO_2/air. The activation

---

*It is probable that sample number 1 was not completely (or identically) cured, and this may have been responsible for the systematic difference in its molecular weight data in all cases.

energies were almost all found to be about 40 to 50 kJ/mol with typical standard deviations of about ±4 kJ/mol. The differences in activation energies with different sample compositions and upon exposure to different gas environments were not found to be significant. One point of note was that the presence of the MNA stabilizer was found to significantly reduce the CL upon exposure to air, but not upon exposure to NO_2/air. (The CL was also not reduced for the sample containing MNA upon exposure to NO but the signal levels were much lower, giving less confidence in the meaning of this observation.) The most surprising difference between these CL data, which can be thought of as a real time aging rate measurement, and the sol/gel and GPC data, which are measurements of the degree of change in binder after an aging period, was for the NO exposure. The NO environment was found to not produce the CL from the polymer. This is reasonable since the conventional reaction mechanism (Refs. 6, 7) for HTPB oxidation involves a radical chain reaction with the two propagation steps:

$$R + O_2 \rightarrow RO_2$$

$$RO_2 + RH \rightarrow RO_2H + R$$

where R represents a polymer radical and RO_2 represents a peroxide molecule. NO has long been used as a radical scavenger in conventional kinetic studies, and if it interrupted the above reaction sequence, the CL, which is generally proposed to be produced from peroxide recombination, would be reduced. The radical propagation chain also requires the presence of O_2. Thus the binder would be expected to exhibit less oxidation upon exposure to NO than upon exposure to air or NO_2/air. The binder reactivity results, discussed above, however, show more or at least as much weight gain and sol fraction for exposure to NO as for air. The GPC analyses of the binder sols show slightly higher averaged molecular weight values for NO exposure than for air or NO_2/air exposure.

The results of this program demonstrate the ability of the real-time chemiluminescence NO_x offgas analysis technique to measure low temperature kinetic parameters important to understanding propellant service lifetimes and the initial stages of propellant combustion. The studies of increasingly complex HTPB-containing mixtures by standard analysis techniques and by a novel solid state chemiluminescence technique contribute important data to help decipher HTPB-containing solid propellant aging chemistry. Additional

experimental work is needed using highly sensitive techniques to study binder degradation and further analytical work to understand these and other results and to expand the understanding of the reaction chemistry to other propellant binders.

3. EXPERIMENTAL

The experimental program was divided into two basic types of measurements: those to measure thermal decomposition rate coefficients of pure energetic materials (alone or in combination with propellant ingredients) and those to measure changes in the binder after exposure to reactive gases which are present during storage of propellants. This approach was selected because of the difficulty in unravelling the aging kinetics of complete propellant formulations. This section is divided into three subsections: Chemicals and Binder Formulations, Oxidizer and Plasticizer Tests, and Propellant Reactivity Tests.

3.1 CHEMICALS AND BINDER FORMULATIONS

The majority of propellant components used in this program were supplied by AFRPL. These chemicals included: hexahydro-1,3,5-trinitro-s-triazine (RDX, 200 μm particles shipped/stored under alcohol/water), ammonium perchlorate (AP, 200 μm particles shipped dry), isophorone diisocyanate (IPDI), and methyl-nitroaniline (MNA). Other propellant ingredients, namely, 1,3,5-butanetriol trinitrate (BTTN, Trojan Chemicals, shipped as 80% BTTN in dichloromethane), aluminum powder (≥ 99.8% Al, 20 μm particles, VarlaCoid Chemical Company catalog no. 8646), hydroxy terminated polybutadiene (HTPB Atlantic Richfield Company, lot # 303065 "Poly-bd" R-45M monomer), and triphenyl bismuth (TPB, Alfa Products, catalog no. 17117, purity not given) were purchased to prepare various binder/propellant formulations. The lot analysis of the HTPB monomer was obtained from Atlantic Richfield Company and is reproduced in Appendix A.

The AP, RDX, and BTTN samples were dried before use. The AP was held for two days in a calcium sulfate filled vacuum desiccator which was continuously evacuated using a mechanical pump. The desiccator was then sealed off under vacuum and the AP stored for an additional four days. The dried sample was used immediately for kinetic measurements. RDX was dried under vacuum

(mechanical pump) for two days then transferred to a desiccator filled with calcium sulfate to dry for four days. The dry RDX was then stored in a sealed flask at ≈ 278 K for future use. Dichloromethane was removed from the BTTN sample in two steps. A sample (ca. 15 cm^3) was first sparged in a test tube with dry, filtered air for three hours. The test tube was then heated for 30 h at 323 K. Periodically, the mass of the BTTN sample was measured to follow the weight loss. Initially, the weight loss was ca. 2% per hour. At the end of 30 h, the sample weight loss was ca. 0.1% per hour and was judged free of solvent. After the sample was cooled to room temperature, it was transferred to a sealed bottle and stored at ≈ 278 K prior to use.

The analytical reagents and purities used for sol/gel analyses and gel permeation chromatography, GPC, were: tetrahydrofuran (HPLC grade, Aldrich), ferrous ammonium sulfate (ACS reagent grade, Aldrich), anhydrous sodium sulfate (ACS reagent grade, Aldrich), toluene (ACS reagent grade, Fisher). The activated alumina (F-1 grade, 28 mesh, Alcoa Chemical Products Div.) and silica gel (anhydrous, 6-16 mesh, Matheson Coleman & Bell) were technical grades. Nitric oxide (99+ %), and an ammonia/nitrogen calibration mixture (50.5 ppm, v/v) used in the NO/NO_x chemiluminescence monitor experiments were from Matheson Gas Co. The nitrogen carrier gas was boiloff from the liquid (typically O_2 < 3 ppm, H_2O < 3 ppm) and was passed through molecular sieve and $CaSO_4$ drying agent traps. Tetrahydrofuran (THF) was the only solvent which was purified before use in either sol/gel or GPC experiments. The THF was passed through a column of approximately equal beds (ca. 2 cm depth, 12 cm diam) of activated alumina, anhydrous Na_2SO_4, silica gel, and ferrous ammonium sulfate. The THF was stored over silica gel and copper wire under nitrogen until use.

Seven "propellant" mixtures containing the HTPB binder were prepared to investigate the ingredient interactions with reactive gases. The composition of these mixtures is given in Table 1. These formulations were prepared by weighing each ingredient as it was added to a 150 cm^3 glass beaker on a top loading balance (Fisher-Ainsworth MX-300, 0.01 g sensitivity). The contents were mixed with a glass stirring rod and then the beaker placed inside a vacuum desiccator attached to a water aspirator. The vacuum was applied and released several times to disrupt the foam which formed and then the vacuum was continuously applied for an additional 30 min. The degassed mixture was

poured into a Teflon tube (1.3 cm i.d., 15 cm length), which was plugged at one end with a cut-off Pyrex test tube, and placed into an oven at 330 K (57°C) for a curing period of 10 days. The oven was purged continuously with nitrogen during the entire curing period. After 10 days, the sample tubes were removed from the oven and placed in a large desiccator filled with Drierite. The oesiccator was flushed with dry nitrogen and stored in a refrigerator held at ≈ 278 K.

TABLE 1

COMPOSITION OF PROPELLANT TEST MIXTURES

	Composition, Sample No., Weight %						
Component[a]	1	2	3	4	5	6	7
HTPB	92.69	92.65	92.47	92.18	26.44	27.94	20.15
IPDI	7.31	7.30	7.29	7.27	2.08	2.20	1.61
AP	--	--	--	--	71.32	--	38.51
Al	--	--	--	--	--	69.70	39.60
NMA	--	--	0.24	0.24	0.07	0.07	0.05
TPB	--	0.05	--	0.31	0.09	0.09	0.08
TOTAL	100.00	100.00	100.00	100.00	100.00	100.00	100.00
NCO/OH	1.00	1.00	1.00	1.00	1.00	1.00	0.99

[a]The HTPB prepolymer was ARCO supplied R-45M. The IPDI, AP, and MNA were AFRPL supplied. The TPB was from Alfa Products. The Al sample (20 μm, purity ≥ 99.8%) was from VarlaCold Chemical Co.

3.2 OXIDIZER AND PLASTICIZER TESTS

The basic experiment in this work was to measure the real time steady state rates of NO, NO_x, or NH_3 evolution from small samples of RDX, BTTN or AP as a function of temperature using a modified NO_x chemiluminescence monitor. The concentration of evolved NO could be measured directly. To measure the concentrations of NO_x, the sum of the NO and NO_2, the flow of N_2 carrier gas containing the decomposition products from the sample was passed through an

AeroChem thermal converter which converted the NO_2 to NO. Similarly, NH_3 could be measured as NO by addition of oxygen to the carrier stream and then passage through the thermal converter. First order decomposition rate coefficients were calculated as the moles of NO_x produced per mole of energetic material per second.

A diagram of the apparatus, constructed using components of a commercial NO_x monitor, is shown in Fig. 1. Up to four samples, 0.5 to 1.5 g each in open 7.5 cm^3 Kimax weighing bottles, were placed in 20 cm^3 cells machined into the thermostated and insulated aluminum block. The fifth cell was left empty for background measurements. The sample cell block was heated by four resistance elements and its temperature was measured using a calibrated platinum resistance thermometer; the temperature was constant to ± 0.1 K. Atmospheric pressure carrier gas, N_2, metered using calibrated critical flow orifices, passed over each sample at about 2 cm^3/s, and was either vented or sampled, one cell at a time, into the NO_x analyzer using Teflon body solenoid valves. For NO concentration measurements the sampled gas flowed directly into the analyzer reactor where it was mixed with a ≈ 2 cm^3/s flow of about 5% O_3 in O_2 from a high voltage ac discharge ozonator. The analyzer reactor was a gold coated spiral channel machined into an aluminum block, facing the photocathode of a cooled, red sensitive trialkali photomultiplier (Centronics P 4283-BA). The reactor pressure was optimized during calibrations to be typically 6.7 kPa with approximately equal flow rates from the sample and ozonator. For NO_x measurements, the sample gas was passed first through the heated platinum wire thermal converter (ca. 1300 K wire temperature) which reduces NO_2 to NO. The sensitivity of the analyzer to NO and the NO_2 to NO conversion efficiency (greater than 95%) were calibrated frequently using a standard $NO/NO_2/N_2$ mixture. An ammonia calibration gas mixture (50.5 ppm NH_3 in N_2) was used to calibrate the instrument for NH_3 analyses. Carrier gas flow rates were measured often with a bubble flow meter.

The photomultiplier signal, proportional to the NO concentration in the reactor when mixed with excess O_3, was amplified and displayed continuously using a chart recorder, and was also digitized, counted, and stored using a desktop computer (Osborne-1). Background corrections were made by subtracting the measurement on the carrier gas which passed through the empty sample cell from the measurement on each oxidizer sample. A custom data acquisition and

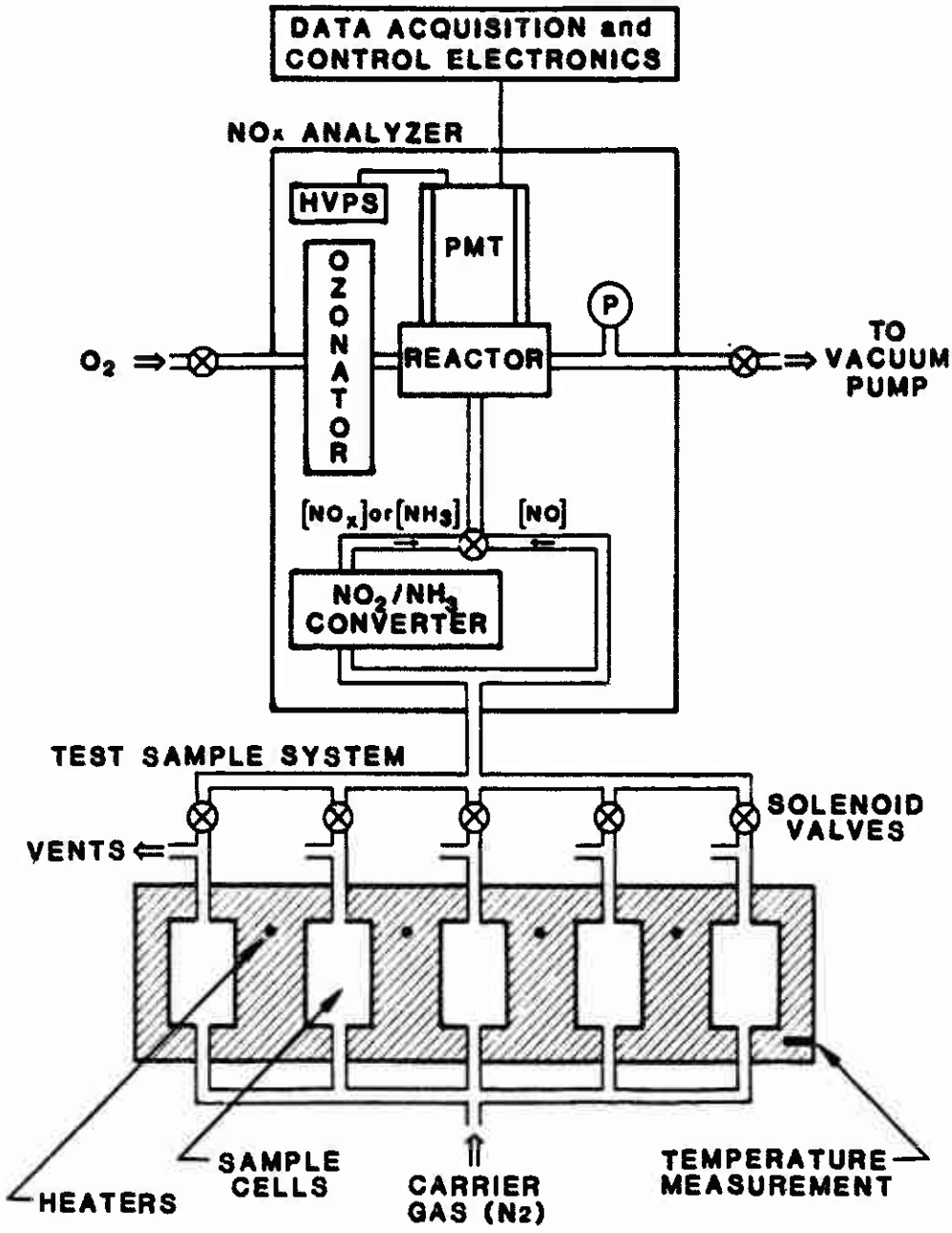

FIGURE 1. NO$_x$ CHEMILUMINESCENCE APPARATUS

control system, shown schematically in Fig. 2, was used to regulate the sample block temperature, perform the data acquisition, and control the solenoid valves which switched the gas flow into the analyzer from sample to background to next sample. The NO_x concentration from the decomposition of the samples was repetitively measured at each temperature until a steady state was achieved, requiring 5 to 10 h or more at the lower temperatures. Figure 3 shows examples of the chart recorder data for NO_x evolution from RDX decomposition at the four indicated temperatures. No complications due to desorption of NO_x from the test samples were encountered.

The thermal stability of RDX precluded direct measurements of the NO_x evolution rates at room temperature. At the lowest temperatures studied, 313-333 K, the flow of nitrogen carrier gas through the sample cells was periodically stopped for 15 min allowing the decomposition products to accumulate. At the end of this period, the nitrogen carrier flow was restarted and the flow sampled by the chemiluminescence monitor. The resulting pulse shaped signal, having a fast rise time and decay, was integrated for about one minute, which was a sufficient time for the signal to return to the steady state background level. The integrated signal was converted into an equivalent NO_x signal by filling a sample cell with the 16 ppm NO_x calibration mixture and repeating the stop flow experiment under identical conditions. Experiments with longer stopped flow times (up to 16 h) were also performed on RDX to determine the amounts of NO_x evolved or adsorbed by RDX samples under storage conditions.

No sample weight loss (i.e., less than 0.0003 g) was measured for RDX or AP samples at the end of a series of experiments covering a temperature range up to 365 K (92°C) and extending over several days. BTTN samples tested above 323 K (50°C) lost a measurable fraction of mass over short time periods and therefore the samples were weighed each day prior to experiments and the rate data were corrected for the mass loss.

Decomposition rate measurements with BTTN were complicated by the presence of BTTN vapor in the carrier gas stream. This problem was solved by inserting a cold trap between the sample cells and the thermal converter. The cold trap was a 3 m long 0.1 cm i.d. Teflon tube, held at either 238 or 195 K (-35 or -78°C). It was established in separate experiments that ≥ 96% of the NO_x in a mixture of 2.5 ppm NO/11.5 ppm NO_2 in N_2 passed through the cold trap

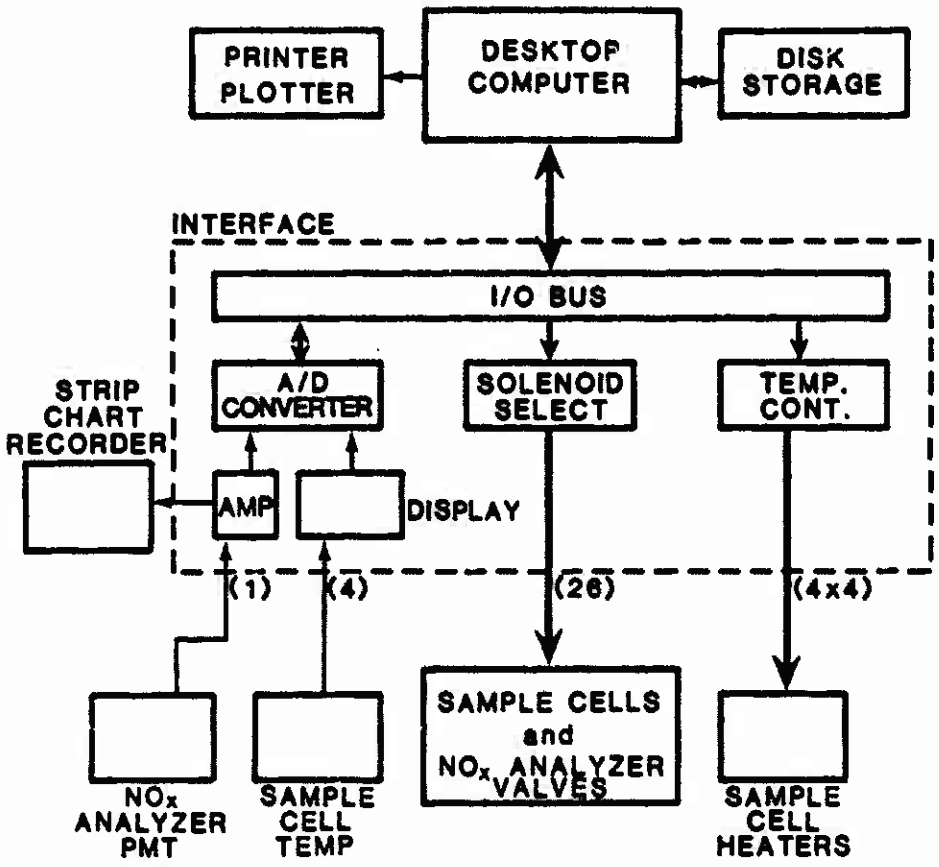

FIGURE 2. DATA ACQUISITION AND CONTROL APPARATUS

The apparatus was designed to manage four sets of four samples.

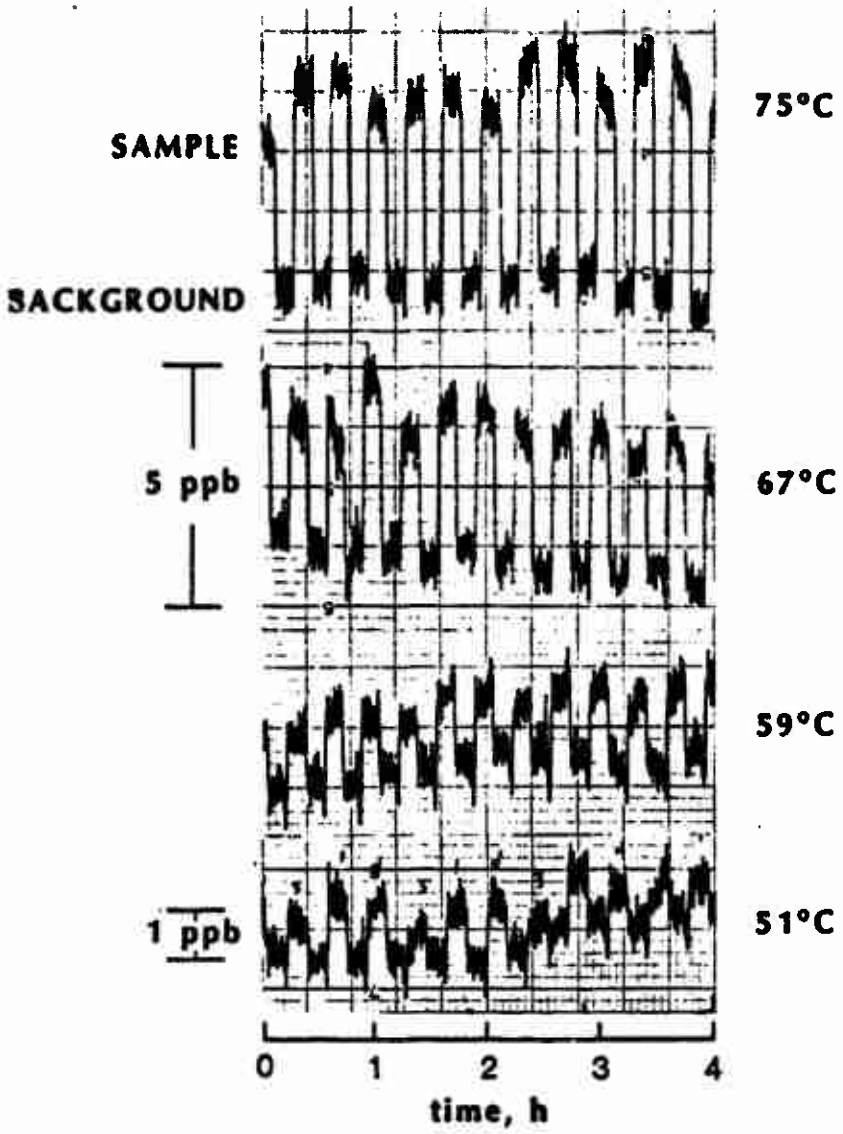

FIGURE 3. REAL TIME NO, CHEMILUMINESCENCE DATA FOR RDX

at 238 K (containing BTTN trapped from decomposition studies). Some material, assumed to be BTTN, was observed to be transported into the cold trap but froze out in the first few cm of the tubing. Periodically the trap tubing was removed from the coolant, warmed (the contents melted), and flushed with acetone and Freon-TF. The procedure insured that no blockage of the gas flow occurred. At no time did we observe transmission of BTTN through the trap.

Ammonium perchlorate decomposition studies were complicated by the release of $HClO_4$ vapors. This problem resulted in nonreproducible NH_3 rate measurements over the 343-393 K (70-120°C) temperature range. This difficulty was solved by adding a Mg turnings filled Teflon tube (0.6 cm o.d., ≈ 10 cm^3 volume) between the samples and the three-way connector at the entrance to the thermal converter. Oxygen, necessary for converting NH_3 to NO, was added through the other arm of this connector. All Teflon lines between the AP samples and the thermal converter, as well as the Mg turning trap, were heated to ≈ 353 K (≈ 80°C) to ensure that NH_3 would not adsorb on the walls. With this modification, the AP decomposition rates were reproducible.

3.3 PROPELLANT REACTIVITY TESTS

These tests included (i) weight gain/loss of binder, sol/gel analysis and gel permeation chromatography (molecular weight distributions) on mixture samples exposed to reactive gases at 344 K (71°C) for 54 h; and (ii) real-time chemiluminescence intensity measurements from samples exposed to reactive gases at several temperatures (303, 313, 333, and 353 K (30, 40, 60 and 80°C)). The first group of measurements will be collectively referred to as "binder reactivity tests" and the second group as "chemiluminescence measurements." All tests were carried out using the propellant mixture series described in the Chemicals and Binder Formulations Section 3.1.

3.3.1 Binder Reactivity Tests

The binder reactivity tests were carried out on samples which were exposed to a reactive gas (mixture). The samples were cut from the Teflon tube containing the binder formulation under study. Using a razor blade, the first 1.0 cm of the 1.3 cm diam tube containing the cured mixture was cut off and discarded. Four discs were then cut from the tube; these discs were 0.2 to 0.6 cm thick and typically weighed between 0.4-0.8 g. Each disc was

then placed in a separate open Kimax weighing dish, and each dish with sample was placed in a sample cell of the chemiluminescence apparatus, Fig. 1. Each sample cell was fitted with a removable Teflon o-ring sealed lid, separate inlet and outlet Teflon lines, and toggle valves. The block temperature was then raised to 313 K (40°C) and the cells were purged overnight with nitrogen. Subsequently, individual cells were purged for ca. 5 min. with one of the reactive gases (N_2, air, NO, or 5.5% NO_2/94.5% air, v/v) and sealed off. The sample block temperature was then raised to 344 K (71°C) for a period of 54 h. The cells were refilled with the respective reactive gas once during this period. At the conclusion of the reaction period, the block was cooled to room temperature and the cells flushed with N_2 for a minimum of one hour. The discs were removed, weighed and immediately subjected to a sol/gel analysis.

The sol/gel analysis began by cutting each binder disc into 0.2 cm cubes and loading the cubes into a test tube with 15 cm^3 of THF. The test tube was capped with aluminum foil and allowed to stand overnight. The test tube contents, solution and gel, were then filtered through a qualitative grade filter paper, the test tube and gel were rinsed with additional THF (ca. 50 cm^3) and the filtrates combined.

If the sample contained AP, the following procedure was employed to remove the small, but significant amount of AP which dissolved in the solvent. The THF filtrates were transferred to a separatory funnel, 10 cm^3 H_2O and 40 cm^3 saturated aqueous KCl solution added, and the contents shaken. The THF fraction was collected and the aqueous fraction was twice additionally extracted with ≈ 30 cm^3 THF aliquots. The combined THF solution was dried over anhydrous Na_2SO_4 for 10-20 min. It was then filtered into a pre-weighed (± 0.1 mg) round bottom flask through a glass fritted funnel loaded with a 3 cm layer of silica gel and a 0.5 cm layer of ferrous ammonium sulfate to remove water and peroxides, respectively. The filter cake was rinsed twice with fresh THF. The receiver flask was placed in a hot water bath and a nitrogen stream was used to remove the solvent. The weight gain of the flask was the sol content of the sample. The weight percent sol (wt% sol) of the sample was calculated as: [(sol content, g) × 100%]/(organic content of sample, g). The organic content of the sample was the mass of all components except the aluminum and ammonium perchlorate.

The sol, a thick yellow oil, was taken up in a few cm^3 of fresh THF, filtered through three Pasteur pipettes (filled respectively with activated alumina, ferrous ammonium sulfate, and silica gel) and a 0.5 μm HPLC membrane filter (Gelman Acrodisc). The sol solution was stored for subsequent molecular weight (MW) analysis by gel permeation chromatography (GPC).

The GPC system used in this work was fashioned after the high performance liquid chromatography (HPLC) apparatus described in the American Society for Testing and Materials (ASTM) publication D 3593-77, Ref. 8, and is shown schematically in Fig. 4. The system components are (ordered according to solvent path, indicated by the arrows in Fig. 4): (a) glass solvent tank with N_2 purge and 3 μm pre-filter; (b) high pressure pump (Milton-Roy Model 396-31); (c) pressure pulse damper (Altex Model 110-40) and pressure resistor (15 m of 0.0178 cm i.d. SS tubing); (d) 0.5 μm filter; (e) pressure gauge (primarily used to detect column blockage); (f) over-pressure relief valve (Rheodyne Model 7037); (g) six-port injection valve (Rheodyne 7010) equipped with 20 μL sample loop; (h) GPC column (25 cm x 0.78 cm i.d., Analytical Sciences Inc., Ultragel linear column) in a thermostated air jacket held at ≈ 306 K (≈ 33°C); (i) sample side of differential refractive index detector, DRID (Knauer Model 98.00); and finally, (j) a 100 cm^3 volumetric flask on a top-loading balance (Fisher-Ainsworth MX-300, 0.01 g readability), which collected the GPC column eluent. A 1 cm^3 sample loading syringe (Hamilton Company, gas tight model #1001) with inline sample filter (a 0.4 cm disc cut from Whatman #4 filter paper) was used to load the sample loop. Initially, pulsations from the single piston pump produced sawtooth fluctuations on the output of the detector even though the pulse dampener was being used. These were eliminated by: (i) daily filling the reference side of the DRID with a static sample of THF instead of continuously pumping solvent through this cell, and (ii) adding the pressure resistor (described above) between the pump and the GPC column. With these modifications, the DRID gave a nonpulsing, nearly flat baseline. Two performance checks, described in ASTM D 3536-76, Ref. 9, were carried out to determine the number of theoretical plates (N), and to measure the resolution (R) of the column. The number of theoretical plates, found by measuring the retention volume and width of the chromatographic peak for $CHCl_3$, was 7500. The ASTM method for determining the MW distributions of polystyrene samples recommends that this value be ≥ 4800. The resolution of the GPC column was

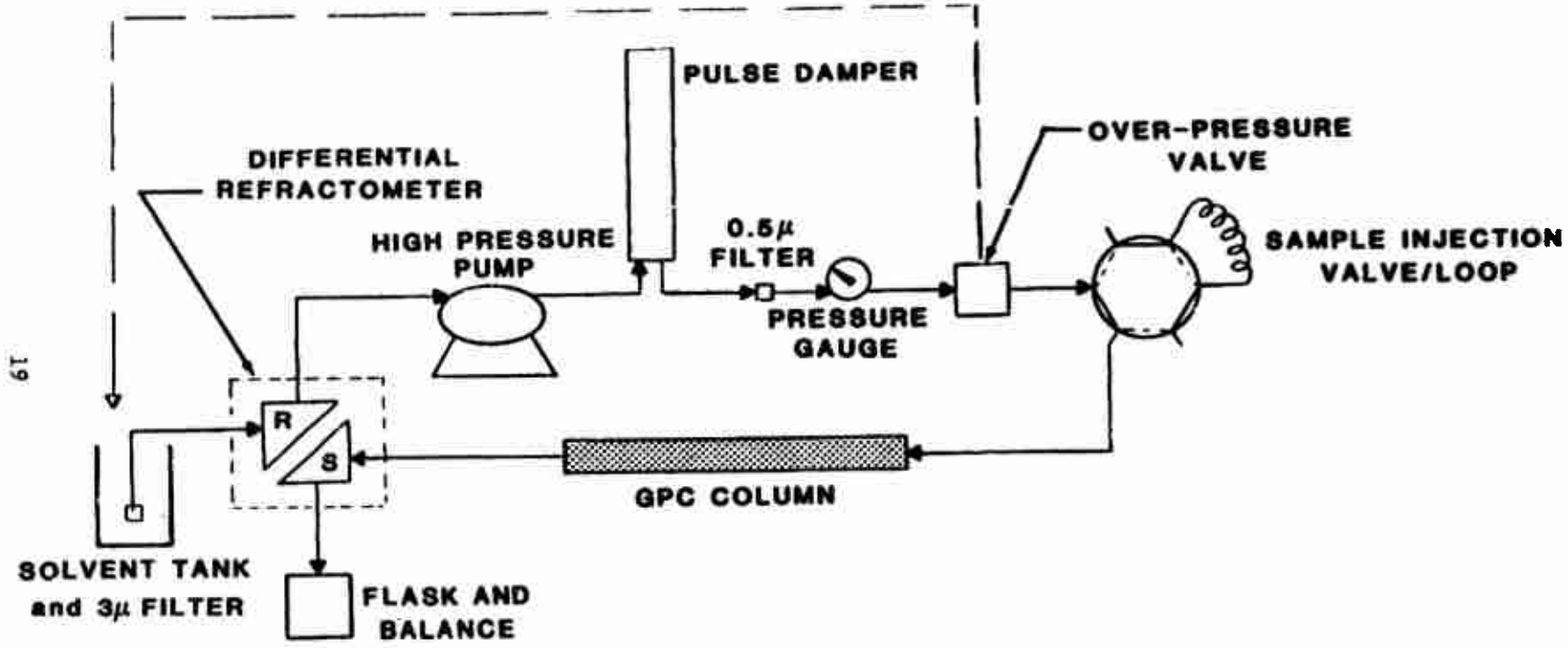

FIGURE 4. GEL PERMEATION CHROMATOGRAPHY APPARATUS

The system was modified to use a static reference cell filled with solvent rather than the flowing path shown.

measured using two narrow MWD polystyrene, PS, standards (Waters Associates). This test measures the ability of the column to separate a mixture containing components of slightly different MWs. The MW data supplied by the manufacturer are reproduced in Table 2. With these two PS standards, the resolution, R, was found to be 2.07. The ASTM method recommends a minimum R of 1.3. Both tests confirm the ability of the short (25 cm length) column to adequately separate the MW components of a mixture of polystyrene.

TABLE 2

MOLECULAR WEIGHT INFORMATION FOR POLYMER STANDARDS

	Molecular Weights			
Polymer[a]	Number Average	Weight Average	Viscosity Average	Peak MW by GPC
PS	4,790	----	2,111	1,800
PS	9,050	----	9,100	8,500
PS	51,150	----	47,400	50,000
PS	92,600	----	98,700	100,000
PS	217,600	----	233,000	240,000
PS	243,000	----	281,000	340,000
PS	790,000	----	----	1,750,000
PB	960	1,027	----	----
PB	22,600	23,600	----	----
PB	135,000	170,000	----	----
PB	206,000	272,000	----	----
PB	286,000	423,000	----	----

[a]Data supplied by manufacturers. Polystyrene (PS) molecular weight standards from Waters Associates. Polybutadiene (PB) molecular weight standards from Scientific Polymer Products. Dashes indicate information not supplied by the manufacturer.

With each GPC chromatogram the cumulative eluent mass was recorded at 1 min intervals. The eluent mass was converted to retention volume using the room temperature density (Ref. 10) of the THF solvent (0.8892 g/cm³ at 293 K). The conversion of the chromatogram peak areas into molecular weight distributions (MWD) required the relationship between retention volume and MW for the specific polymer under analysis. HTPB MW standards were not commercially available. In this program, polybutadiene (PB) MW standards (from Scientific Polymer Products) were used to calibrate the GPC system for PB MWs against retention volumes, assuming that HTPB and PB act similarly in the column. Thiokol/Wasatch (Ref. 11) used another method in which a broad MW distribution HTPB polymer was separated into fractions using GPC prep columns and then the MW of each of the fractions was determined using light scattering, osmometry, or vapor pressure measurements. One difficulty with both approaches is that the PB and HTPB MW standards are easily oxidized in air, so that a single standard is not suitable for calibration over extended periods. Therefore in this work, the GPC column was occasionally calibrated simultaneously with both PB MW and PS MW standards under conditions identical to those used to analyze the propellant sols. The PS standards are stable at room temperature in air. For daily GPC work, the PS MW standards were then used to calibrate the system. To prolong the lifetimes of the PB MW standards, they were stored at ≈ 273 K under nitrogen. Table 2 shows the manufacturer supplied characteristics of both the PB and PS calibration standards. An example of the observed dependence of PS and PB molecular weights on retention volume is shown in Fig. 5. The equation for converting from the daily calibration polystyrene MWs to polybutadiene MWs is: $MW_{PB} = -63.5 + 0.6266 \times MW_{PS} + (8.629 \times 10^{-9}) \times (MW_{PS})^2$. The standard deviation of the fit and chi-square tests gave: $\sigma(fit) = 57$ Daltons, and $\chi^2 = \Sigma(Y_{calc} - Y_{obs})^2 = 22{,}500$ (Dalton)². This empirical relationship was determined, using the PS and PB calibration data, by fitting the data to the form $\ln[MW] = a + b \times V_R$, where V_R was the observed GPC retention volume in cm³. For PS molecular weight standards, the least squares analysis gave: $\ln(MW_{PS}) = 25.834 - 2.474 \times Vr$ ($r^2 = 0.999$; data point for MW = 1,750,000 excluded). For PB molecular weight standards, least squares analysis gave: $\ln(MW_{PB}) = 25.441 - 2.487 \times Vr$ ($r^2 = 0.990$). The calculated MWs are correlated with one another, resulting in the quadratic function given above.

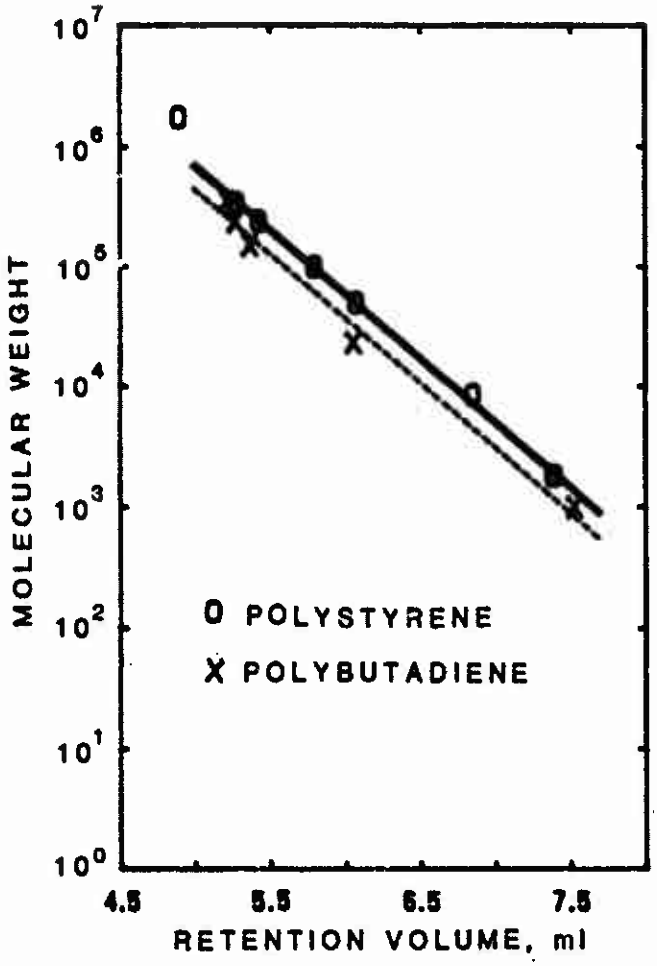

FIGURE 5. GPC MOLECULAR WEIGHT CALIBRATION CURVE

A computer program was developed and used to convert the analog chromatogram of each propellant sol to polybutadiene MWs using the PS to PB molecular weight relationship and daily calibrations. An electronic digitizer pad (GTCO Corp., 0.0025 cm resolution) was used to input the strip chart data into a BASIC computer program. The computer program: (1) generated the "polystyrene MW" vs. retention volume calibration equation; (2) converted from retention volumes to "polybutadiene MWs"; and (3) performed the calculations listed in the ASTM procedures to obtain the MWDs. In addition, this program calculated the resolution and number of theoretical plates for the GPC column (useful information for gauging the performance of the columns), corrected for baseline shifts, corrected for the true mass flow rate through the column, and calculated the number average MW and weight average MW for the sol according to the ASTM procedure D 3593-77, Ref. 8.

3.3.2 Chemiluminescence Measurements

The apparatus for measuring the chemiluminescence light intensity from a propellant sample exposed to reactive gases at fixed temperatures, is shown in Fig. 6. This apparatus was modelled after the system used (Ref. 2) at SRI.

Critical flow orifices were used to meter the reagent gases. The reagent gas (40-100 cm^3/s) passed through a 30,000 cm^3 mixing chamber before entering the CL apparatus. Each sample (1.3 cm diam, 0.2-0.4 cm thick) for a CL study was cut from one of the Teflon tubes containing the propellant mixtures. The sample in a Kimax dish was placed on the heated (8.9 cm diam, 304 stainless steel) platform in the center of the sample chamber. The temperature of the platform was monitored using a digital readout (Omega Model 199) and a K-type thermocouple located in a well on the underside of the platform. The heater current was controlled by an a.c. temperature regulator (Oven Industries Model 5CX 220P). The long and short term temperature stability of the heating system was ± 0.5 K. The heating system responded to a temperature increase of 20 K with a 4 to 5 min time constant.

The detection system consisting of a quartz window, collimator, shutter, and a cooled photomultiplier detector (EMI 9558 QB in a Products For Research housing Model TE-104) was mounted on the o-ring sealed top plate. An evacuated quartz cell located in front of the photomultiplier prevented

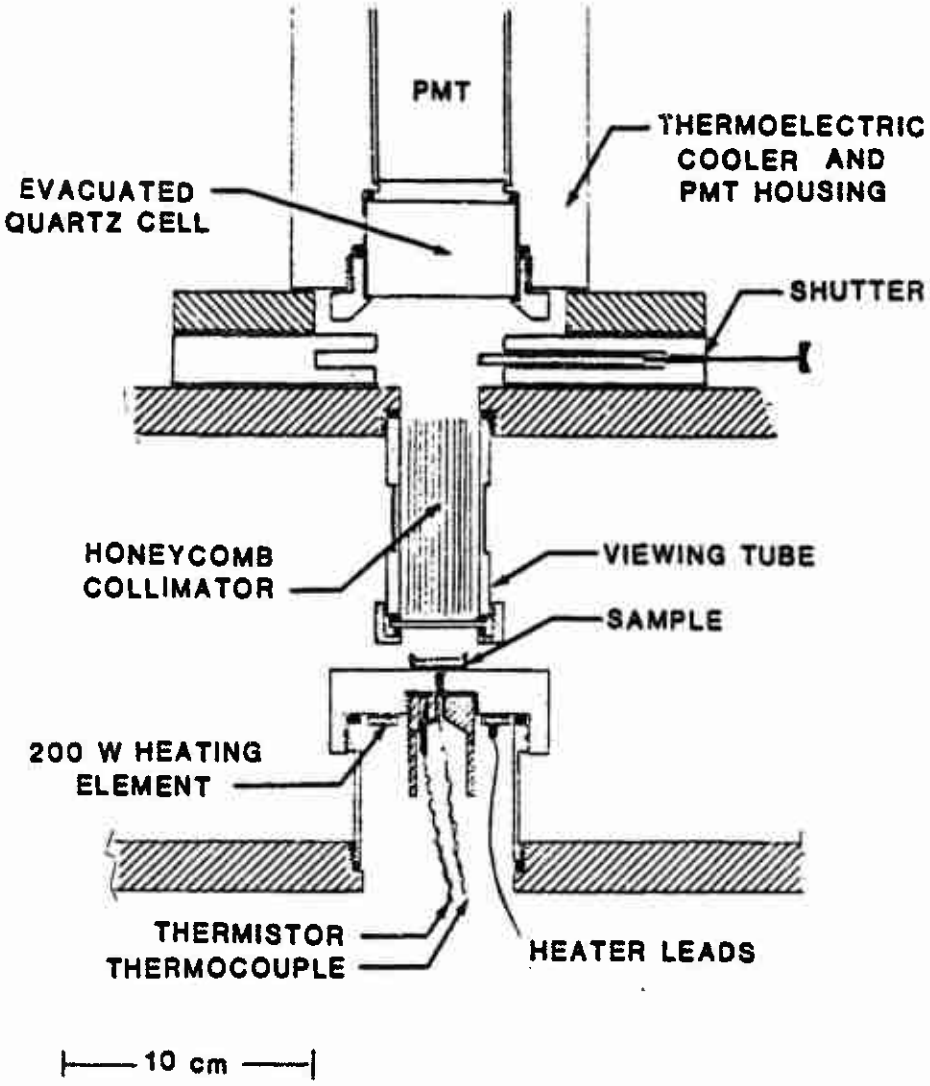

FIGURE 6. POLYMER CHEMILUMINESCENCE APPARATUS

condensation or frost buildup on it. The photomultiplier was operated at -1400 V and the output current pulses were routed to a multichannel scaler (MCS) (Canberra Industries, Inc. Model 35). The MCS counted the number of pulses from the photomultiplier larger than a preset discriminator level and stored the count in time-sequenced channels. The number of counts per channel is proportional to the intensity (photons/cm^2/s) of the chemiluminescence at the low light levels of these measurements. Response is linear for pulse separation $\geq$ 50 μs (i.e., $\leq$ 20,000 pulses/s). The highest pulse rate with a zero discriminator level and counting the pulses from a HTPB binder sample at room temperature in nitrogen was $\approx$ 10,000 per second. Thus no significant nonlinearity errors were expected due to near simultaneous pulses.

The discriminator level was determined experimentally by comparing the pulse height distributions with and without CL. At small pulse amplitude, the number of background and dark current noise pulses was nearly identical to the number of pulses from the sample CL as shown in Fig. 7. The discriminator level was set just above the pulse amplitude where the two pulse height distributions differed ($\approx$ 3 amplitude units on the scale of Fig. 7). The background count rate (in the absence of propellant sample) varied with room temperature and sample holder temperature, but was independent of reagent gas as shown in Table 3.

For measurements, a sample disc was loaded and it and the CL apparatus were purged with a nitrogen flow for 30 min. The temperature was then increased to 359 K (86°C) for 24 h with nitrogen flowing. After this cycle (during which additional cure reactions probably occurred), the heater was turned off and the sample was allowed to cool to room temperature. The reagent gas flow through the CL apparatus was started (either N_2 at 40 STP cm^3/s flow rate, air at 100 cm^3/s, 1 cm^3/s NO + 40 cm^3/s N_2, or 1 cm^3/s NO + 100 cm^3/s air). For approximately 30-60 min, the dark count rate (i.e., shutter closed) was recorded using a 60 s MCS channel width. Then the shutter was opened, the sample heater turned on, and CL from the sample analyzed at 303 K (30°C) for $\approx$ 1 h. The shutter was then again closed and dark count recorded. This cycle was repeated for each of the temperatures under study in increasing order, 303, 313, 333, and 353 K. The data were then transferred from the memory of the MCS to a desktop computer for analysis. This analysis involved fitting the dark count rate to a polynomial equation, usually a quadratic, and

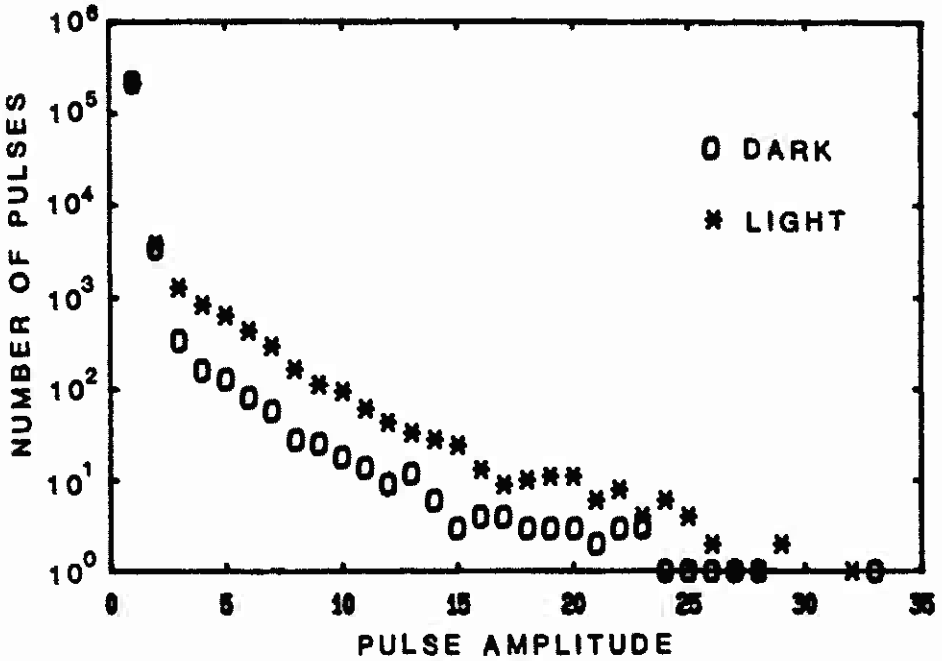

FIGURE 7. PULSE HEIGHT DISTRIBUTION OF POLYMER CHEMILUMINESCENCE AND BACKGROUND SIGNAL

TABLE 3

CHEMILUMINESCENCE SIGNALS (COUNTS PER MIN) FROM EMPTY APPARATUS

	Sample Holder Temperature[a]	
Gas	30°C	90°C
Dark Count	2986 ± 52	3734 ± 82
N_2	2977 ± 103	3544 ± 52
NO/N_2	2943 ± 49	3642 ± 84
Air	2996 ± 54	3576 ± 88
NO_2/air	2994 ± 49	3680 ± 102

[a]Errors represent the standard deviation of eight, one minute counting periods.

subtracting the polynomial estimate of the dark count from each data channel. The CL data, thus corrected to a zero baseline, were grouped according to the sample temperature, and the average and standard deviations were calculated for: (a) all the channels of the temperature group, and (b) the first few channels of the temperature group (where usually the peak CL count was observed). The averaged values at each temperature were then used to determine the variation of the CL intensity as a function of temperature.

The above procedure was repeated for each reagent gas using a fresh propellant sample. The 24 h cycle in nitrogen at 359 K prior to experiments and the use of a fresh sample disc with each reactive gas were necessary to obtain reproducible CL data. The reproducibility is illustrated in Table 4 for three discs cut from sample mixture 1.

TABLE 4

FITTING PARAMETERS[a] FOR CL FROM THREE DISCS OF SAMPLE 1 IN NITROGEN

Disc No.	Trial No.	"a" Parameter counts/min	Activation Energy kJ/mol
1	1	11.92 ± 0.26	57.9 ± 1.7
	2	11.45 ± 0.04	54.5 ± 0.2
2	1	11.62 ± 0.09	57.4 ± 0.6
	2	10.87 ± 0.16	52.3 ± 1.0
3	1	10.88 ± 0.65	52.1 ± 4.4
	2	10.85 ± 0.19	51.6 ± 1.3

[a]The fitting equation was: counts/min = $10^a \times \exp(-Ea/RT)$. The error bars indicate one standard deviation in the uncertainty of the fitting parameters.

A considerable amount of initial polymer chemiluminescence work was performed until systematic procedures were developed and several problems solved. Early experiments were performed on binders cured at 330 K for ten days in air, after which they were placed in a room temperature, air filled desiccator for long term storage. With some samples, the NO/N_2 gas environment resulted

in a larger CL intensity than from N_2. In all previous preliminary tests the N_2 environment resulted in a similar or larger CL signal than NO/N_2. This difference probably occurred because of reaction of NO with oxygen trapped in the binder during the curing process in air, generating in situ NO_2. Furthermore, these air-cured samples required much longer times for the CL signal to reach steady-state plateaus. We think that some of these samples were not completely cured and that they further cured at the higher test temperatures. This resulted in sets of CL data dependent on sample history.

These data strongly suggested that the binders used in CL experiments needed to be fully cured if reliable and repeatable CL data were to be obtained, and that the O_2 from air processing of the samples had to be removed by degassing, curing in N_2, and minimal handling in air. Thereafter, the samples were stored in refrigerated dry nitrogen after curing and handled with minimal contact with air. A new sample slice was used for measurements on each different reactive gas but data for the four temperatures for each gas environment were obtained using one slice. Duplicate samples were run.

4. RESULTS AND DISCUSSION

4.1 OXIDIZER AND PLASTICIZER DECOMPOSITION KINETICS

4.1.1 RDX Decomposition

The thermal decomposition of the practically important nitramine, hexahydro-1,3,5-trinitro-s-triazine (RDX or cyclotrimethylene trinitramine) has previously been extensively studied most successfully near its melting point at 477 K, yet controversy still exists about the mechanism of the initial decomposition step. Little reliable kinetic data are available (Ref. 3) for temperatures below about 450 K. The many previous studies of the mechanism and kinetics of the thermal decomposition of RDX have been extensively discussed in several comprehensive reviews (Refs. 3, 12, 13). When studied in a closed, small volume system the secondary reactions of the gaseous decomposition products with each other and with the RDX itself are of primary importance (Ref. 14) and cloud the identity of the primary decomposition step. There is evidence (Refs. 15, 16) that both gas phase and condensed phase decomposition processes are important at 468 K. Recent work by Oyumi

and Brill, Refs. 17 and 18, using rapid heating and time-resolved infrared spectroscopic techniques appears to have established that NO_2 is the predominant initial gaseous decomposition product, even though it later disappears due to secondary reactions. Oyumi and Brill also found that little NO was initially formed, HONO was present in small quantities early in the reaction, and gas phase and solid phase decomposition products were observed at low and high pressures, respectively.

The thermal decomposition of RDX in the liquid phase near its melting point has been characterized (Refs. 3, 12) by a rate coefficient, $k = 10^{19.5} \exp[-24{,}410/T)]\ s^{-1}$, thus having an activation energy, Ea, of 202.9 kJ/mol. In the gas phase, the preexponential factor was smaller, $10^{13.5}$, and the activation energy was 142.7 kJ/mol. For solid phase RDX, Fifer, Ref. 3, concluded that no reliable rate data were available due to the complications of autocatalysis and sublimation. Cosgrove and Owen, Ref. 15, proposed that the products observed in their experiments using solid RDX at 468 K were, in fact, due to the decomposition of the molecules in the vapor phase above their solid sample, and that the rate coefficient for solid phase decomposition was smaller than for the gas or liquid phase.

The basic experiment in this work was to measure the real time steady state rates of NO or NO_x evolution from small RDX samples as a function of temperature using a NO/O_3 chemiluminescence monitor. The concentration of NO was measured directly. To measure the sum of the concentrations of NO and NO_2, the flow of N_2 carrier gas containing the decomposition products from the sample was passed through a thermal converter. First order decomposition rate coefficients were calculated as the moles of NO_x produced per mole of RDX per second.

NO_x evolution rates from RDX were measured over the temperature range from 332 to 375 K, and the first order decomposition rate coefficients are shown in Arrhenius form by the circles in Fig. 8. Stopped flow measurements, shown by the triangles in Fig. 8, were obtained at three temperatures between 316 and 332 K. The numerical rate coefficient data are given in Table 5. The error limits shown in the figure are one standard deviation from the average rate coefficient determined for the three RDX samples. Rate coefficients determined for any individual sample were more precise. The error limits for the higher temperature data lie within the bounds of the circles in the

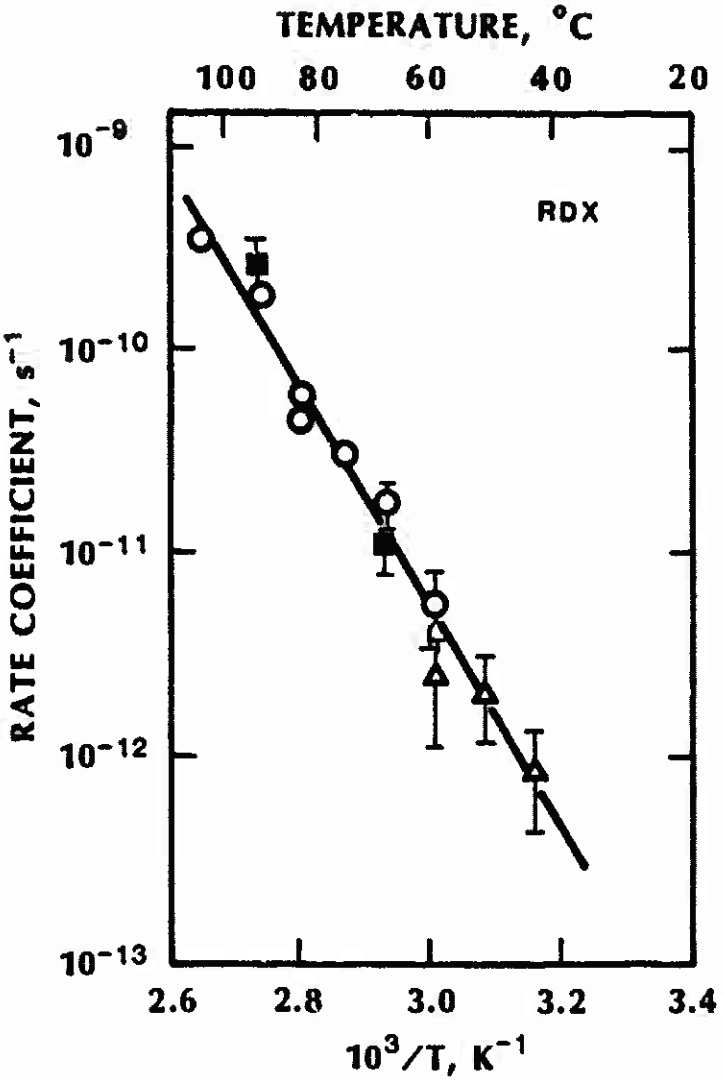

FIGURE 8. ARRHENIUS GRAPH OF RDX DECOMPOSITION DATA

○ = Real time data; ■ = real time data using cold trap; △ = data obtained from 15 min accumulations.

TABLE 5

DECOMPOSITION RATE COEFFICIENTS FOR RDX

Temperature		NO_x Rate Coefficient[a]	NO_x concentration
°C	K	k, 10^{-10} s^{-1}	ppb
59.2	332.4	0.058 ± 0.024	0.23 ± 0.10
67.2	340.4	0.179 ± 0.048	0.72 ± 0.13
75.2	348.4	0.311 ± 0.044	1.20 ± 0.22
83.1	356.3	0.459 ± 0.063	1.78 ± 0.34
83.1	356.3	0.623 ± 0.057	2.41 ± 0.31
91.1	364.3	1.89 ± 0.25	7.30 ± 1.31
103.1	376.3	3.64 ± 0.33	14.1 ± 2.1
42.2	316.4	0.0092 ± 0.0049[b]	---
51.2	324.4	0.022 ± 0.010[b]	---
59.2	332.4	0.025 ± 0.014[b]	---
67.2	340.4	0.110 ± 0.034[c]	---
91.1	364.3	2.20 ± 0.50[c]	---

[a]The error bars are due to sample to sample variability. Measurements of the rate coefficients for single RDX samples were more accurate.

[b]Derived from 15 min stopped flow experiments.

[c]Data obtained using 238 K (-35°C) cold trap.

TABLE 6

COMPARISON OF NO AND NO_x EVOLUTION FROM RDX

Temperature		[NO_x]	[NO]	
°C	K	ppb	ppb	NO/NO_x Ratio
71.3	344.5	---	0.39	---
75.2	348.4	1.3	0.56	0.46
79.3	352.5	---	1.0	---
87.2	360.4	4.7	---	---
87.3	360.5	4.4	2.5	0.55
91.3	364.5	7.9	3.4	0.44

figure. The combined data set was fit (using a nonlinear least squares algorithm with individual data points weighted by their variance) by the expression $k = 10^{4.9 \pm 0.5} \exp(-12,430 \pm 700/T)\ s^{-1}$ from 316 to 376 K (43 to 103°C). An activation energy of 103.3 ± 5.8 kJ/mol was obtained. Measurements of NO evolution rates (without using the thermal converter) from 340 to 360 K indicated that roughly equal amounts of NO and NO_2 were present in the evolved gases (i.e., $NO/NO_x \sim 1/2$, see Table 6). Similar activation energies were found for both the NO and NO_x measurements. Previous work (Ref. 4) on nitrocellulose decomposition in a similar apparatus and under similar conditions of temperature and concentration showed that a considerable fraction of the NO_2 can be rapidly reduced to NO by secondary reactions, probably with the nitrocellulose in that work. Thus it was not surprising to observe significant quantities of NO in the decomposition products from RDX in these experiments, but NO_2 was assumed to be the primary product as supported by the work of Oyumi and Brill, Ref. 17.

Two additional experiments were later performed with a dry ice/isopropanol cold trap (238 K, -35°C) between the samples and the NO_x analyzer to confirm that no condensables, such as RDX vapor, were being carried into the reactor or converter and decomposed to give an anomalous NO_x signal. That neither NO nor NO_2 were lost in this trap was confirmed using the calibration gas mixture. The RDX decomposition rate coefficients obtained using this cold trap were indistinguishable, to within the uncertainty of the data, from those obtained without the trap. These data points are shown in Fig. 8 and Table 5.

The concentration of NO_x which was observed to build up above a RDX sample in a sealed sample cell with no carrier gas flow is shown in Fig. 9 and Table 7 for two temperatures. Prior to making these measurements, each cell (both sample cells and the empty reference cell) was filled with a 250 ppm NO_x in N_2 mixture and sealed off for one hour to "season" the surfaces. The cells were then purged overnight with N_2 and used for accumulation rate experiments. This procedure increased the reproducibility of the data. Each point in Fig. 9 represents the average of six measurements. The overall rate of NO_x production decreased with time and the concentration was observed to reach a plateau value after about 10 h. Since the conversion of NO_2 to NO would not change the value of the measured NO_x signal, these curves indicate either a decrease

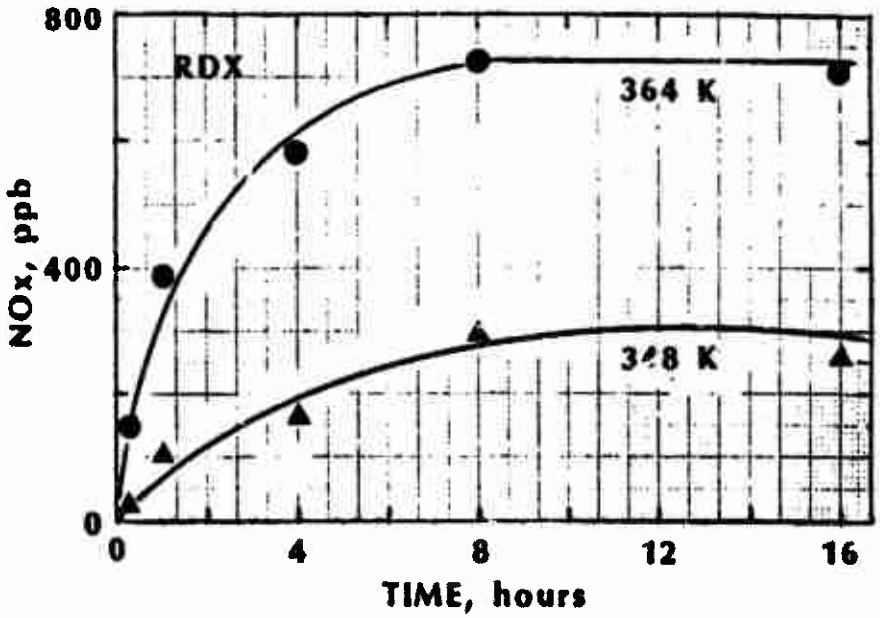

FIGURE 9. LONG TERM ACCUMULATION OF NO_x FROM RDX DECOMPOSITION

TABLE 7

NO_x CONCENTRATION MEASUREMENTS FOR 1 g RDX SAMPLES UNDER TWO STORAGE CONDITIONS

Storage Time, min	NO_x Concentration,[a] ppb 348.4 K	364.4 K
15	27 ± 12	151 ± 30
60	108 ± 34	386 ± 97
240	163 ± 66	577 ± 110
480	296 ± 140	724 ± 200
960	254 ± 174	712 ± 266

[a]The tabulated values are the average and standard deviations of six measurements (two samples, three trials each).

in the production rate of NO_x (negative autocatalysis) or the loss of NO_x due to secondary reactions or adsorption.

Considering the steady state NO_x concentrations as simply the result of equality of the NO_x production rate (as quantified by k [RDX] with the expression for k given above) and a surface rate of NO_x removal (rate given by k(rem) A $[NO_x]$, where A was the RDX surface area and $[NO_x]$ was the observed steady state NO_x concentration), an analysis for k(rem) was performed. The surface area of this 200 μm RDX was measured using a one point N_2 BET analyzer to be 0.30 m^2/g and absorption of NO_x on the cell walls was ignored. Thus, k(rem) = (k [RDX])/(A $[NO_x]$), yielded values of k(rem) of 4.9×10^{-6} at 348.4 K and 9.3×10^{-6} at 364.4 K. The activation energy of this removal process was estimated from these two points to be 46.4 kJ/mol. Although this Ea value is larger than for most physical adsorptions, first monolayer adsorption can exhibit an activation energy as large as 30 to 38 kJ/mol (Ref. 19). We conclude that the process responsible for the leveling off of the NO_x concentrations was probably chemi-adsorption, but a simple physical absorption process cannot be eliminated. Further analysis of this process, such as measurements of the heats of absorption, was beyond our scope of work, but should be pursued to shed further light on the reaction mechanism.

Cosgrove and Owen, Ref. 15, proposed that the products observed in their experiments using solid RDX at 468 K were, in fact, due to the decomposition of the molecules in the vapor phase above their solid sample, and that the rate coefficient for the solid phase decomposition was smaller than for the gas or liquid phase. The results from our real time thermal decomposition measurements are not consistent with decomposition of RDX vapor to produce the observed NO_x at temperatures up to about 380 K. This was demonstrated in two ways. First, no difference in NO_x concentration was observed with or without a 238 K (-35°C) trap between the samples and the thermal converter. All of the RDX vapor carried out of the reaction cell by the inert gas flow would have been decomposed to give NO_x in the converter. Second, it was assumed as an upper limit, that an equilibrium vapor pressure (Ref. 20) of RDX existed in the sample cells, and a decomposition rate coefficient was calculated attributing the observed NO_x in our experiments to decomposition of this vapor. The rate coefficients thus calculated were 10^5 to 10^{10} larger than the gas phase value of Rodgers and Daub, Ref. 21. This does not, however, mean that

decomposition of vapor phase RDX could not be important in experiments carried out by others at higher temperatures where both the rate coefficients and vapor pressures are many orders of magnitude larger than under our low temperature conditions. If the (extrapolated) solid phase decomposition rate coefficient from this work, the gas phase rate coefficient (Ref. 21), and the reported vapor pressure data (Ref. 20) are used to calculate the competing solid and gas phase rates of decomposition of RDX under the conditions of Cosgrove and Owen (0.2 g of RDX in a 150 cm^3 reactor at 468 K), the gas phase process is, indeed, found to dominate the production of reaction products by greater than a factor of 100. Thus although the vapor decomposition made no contribution to the NO_x concentrations measured in this work, the present results, when extrapolated to temperatures near the melting point of RDX, show that the contribution to NO_x concentrations from the vapor decomposition can dominate that from the solid.

The mechanistic interpretation of the Arrhenius parameters obtained in this work is not clear. Figure 10 shows a comparison of the recommended (Refs. 3, 12) higher temperature rate coefficients for liquid and gas phase RDX along with the results of this work. The solid line representing the current data has been extrapolated (dashed line) down to room temperature where the calculated value was 3×10^{-14} s^{-1}, demonstrating that RDX is very stable under ambient conditions. At 298 K, RDX has a half life of $\approx 6 \times 10^5$ years and is, for example, about 50 times more stable than nitrocellulose (Ref. 4). The rate coefficient extrapolated to just below the melting point, 450 K, is about a factor of 10 smaller than earlier rough estimates (Ref. 3) of the solid phase upper limit of 1×10^{-6} s^{-1}. Considering the uncertainties in previous solid phase determinations due to sublimation or catalytic effects, the upper limit estimate (Ref. 3) is in excellent agreement with the extrapolated rate coefficient value from this work. The activation energy for solid phase RDX decomposition, 103 kJ/mol, is considerably smaller (Ref. 22) than the activation energy for gas phase $N-NO_2$ cleavage in other molecules, but it is only slightly lower than the Ea for gas phase decomposition (Ref. 3) of RDX, 128 kJ/mol.

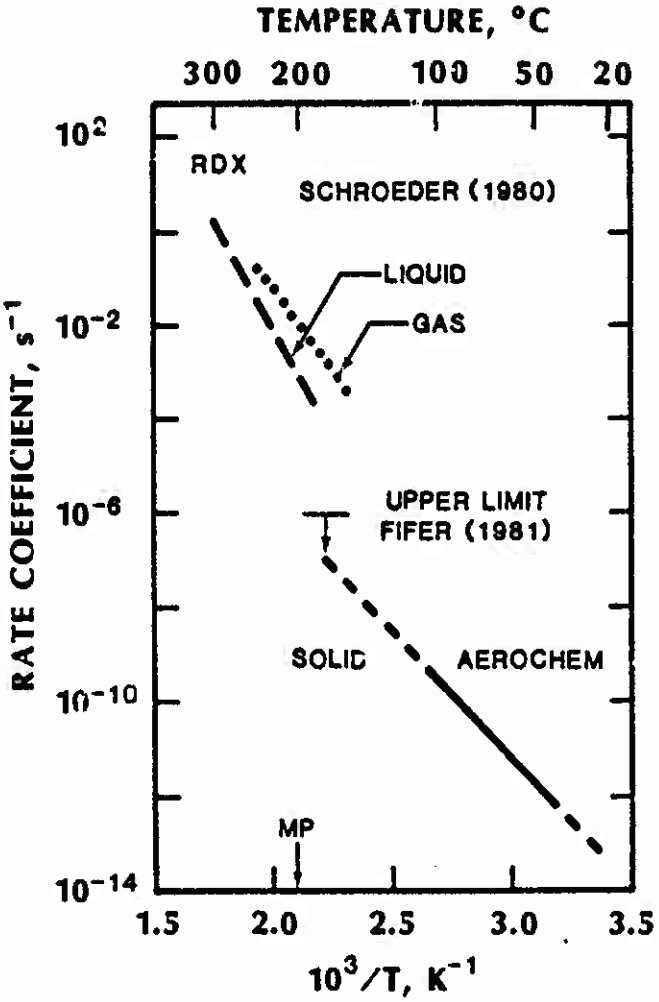

FIGURE 10. COMPARISON OF RDX DECOMPOSITION RATE COEFFICIENTS

4.1.2 AP Decomposition Kinetics

The measurements of AP decomposition were performed using generally the same apparatus and procedures as used for RDX. The carrier gas was changed to air, needed to convert the NH_3 to NO catalytically, and an oven was added to heat all of the delivery lines uniformly to about 353 K (80°C) to prevent NH_3 adsorption (almost all of the NH_3 adsorbed onto the surfaces until the lines were heated to above 333 K (60°C)). Also a strongly interfering species was found to be present in the stream carrying the decomposition products; the species was assumed to be perchloric acid vapor. The interference was eliminated by adding a scrubber containing magnesium turnings to remove the acid. A calibration of the instrument sensitivity to NH_3 was performed by flowing a commercial mixture of 50.5 ppm NH_3 in N_2 (Matheson Gas Co.) into a 500 cm^3 mixing bottle along with a stream of air. The flow rates of both streams were metered using calibrated orifices. The mixture exiting from the bottle was sampled into the NO_x analyzer through the thermal converter using the same lines and apparatus conditions as used for the AP decomposition experiments. An efficiency of 84 ± 5% was found for the measurement of NH_3.

With these modifications, reproducible NH_3 evolution rates from AP decomposition were obtained at four temperatures between 343 and 378 K, down to our real time limit of NH_3 detection of about 0.4 ppb. These data were analyzed to determine the thermal decomposition rate coefficient of AP as shown in Table 8. Over the temperature range of 344 to 380 K (71 to 107°C), the data were fit to the Arrhenius expression: $k = 3.45 \times 10^7 \exp[-(14,900 \pm 200)/T]\ s^{-1}$ as shown in Fig. 11. The activation energy, 123.8 ± 17.2 kJ/mol, was in good agreement with earlier Ea values obtained at higher temperatures below the cubic to orthorhombic phase transition at 513 K of 142 (Ref. 23), 105 (Ref. 24), and 126 kJ/mol (Ref. 25) as shown in Fig. 12. We have chosen to compare the present data with data analyzed using the Avrami-Erofeev kinetic model (Ref. 23) which we consider to be the most reliable. Even so, there was an uncertainty in the derived rate coefficients due to the uncertainty in the value of the stoichiometry parameter "n" assumed in each reference (values of 1.5-2.0 were used). Though the activation energies agree approximately, the present rate coefficient values are lower by about a factor of 10 to 30 than the (nearly six decade') extrapolation to 363 K of those previous rate coefficient expressions. These previously measured rate coefficients differ

TABLE 8

DECOMPOSITION RATE COEFFICIENTS FOR AP

Temperature °C	Temperature K	Rate Coefficients[a] 10^{-10} s^{-1}	$[NH_3]$, ppb
71.4	344.6	0.049 ± 0.011	0.42 ± 0.20
79.4	352.6	0.162 ± 0.049	1.40 ± 0.28
91.2	364.4	0.788 ± 0.136	6.85 ± 0.96
107.2	380.4	2.82 ± 0.67	24.5 ± 5.5

[a]The error limits are one standard deviation for data obtained on four 1.2 g AP samples at each temperature.

among themselves by more than a factor of 10 at about 475 K. (The literature on the chemistry of AP decomposition will not be extensively discussed here. See Ref. 26 for a general review and other references.) There are no rate data from temperatures near those of our experiments against which to compare. Extrapolation of the rate coefficient expression derived in this work to room temperature yields a value of $k(300\ K) = 9.4 \times 10^{-15}\ s^{-1}$, demonstrating the high stability of AP.

Experiments were also performed to investigate the effect of other propellant ingredients on the rate of NH_3 evolution from AP decomposition. Measurements on two samples, 50/50 (wt%) AP/Al and repeat measurements on pure AP (using fresh AP), were carried out as described above. The AP was from AFRPL (200 μm particles) and the Al was from VarlaCoid Chemical Company (≥ 99.8% purity, 20 μm particles). Ammonia evolution rates were measured over the temperature range 356-380 K (83-107°C) and are presented in Table 9 and Fig. 13. The AP/Al NH_3 evolution rate coefficients appear to be slightly higher than those of the pure AP (Table 9) but, within the error limits of each data set, all three sets of rate coefficients are identical. We conclude that the Al does not noticeably affect the AP decomposition rate.

The final test in this series was to measure the NH_3 evolution rate from a mixture of 49.7% AP in HTPB/IPDI (NCO/OH = 1.00). About 1.5 g of this mixture was cast into each of three weighing bottles for these tests. The NH_3 evolution from these films may have been limited by the time required for

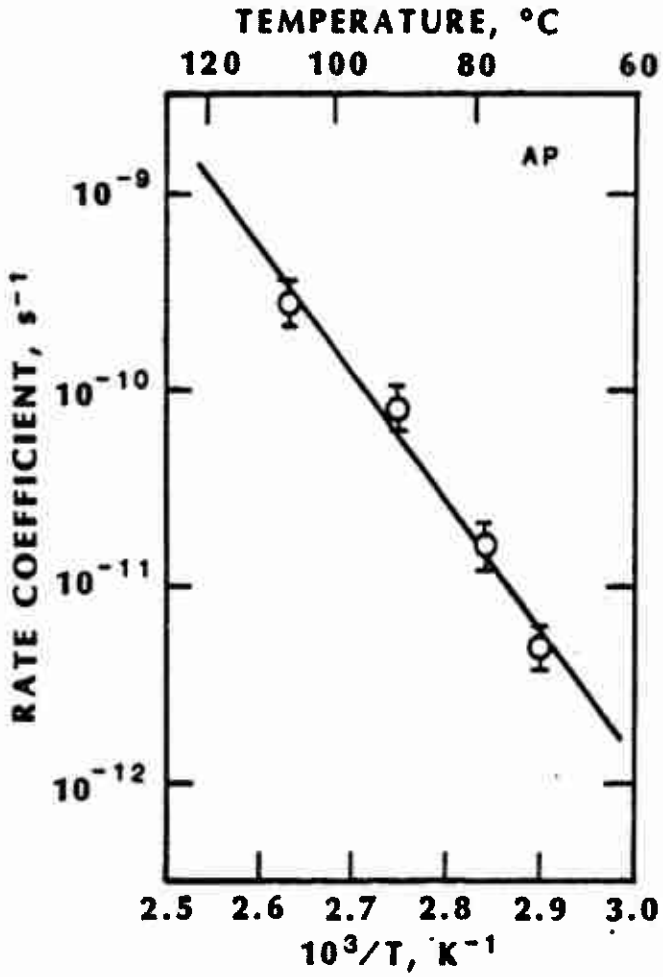

FIGURE 11. ARRHENIUS GRAPH OF AP DECOMPOSITION DATA

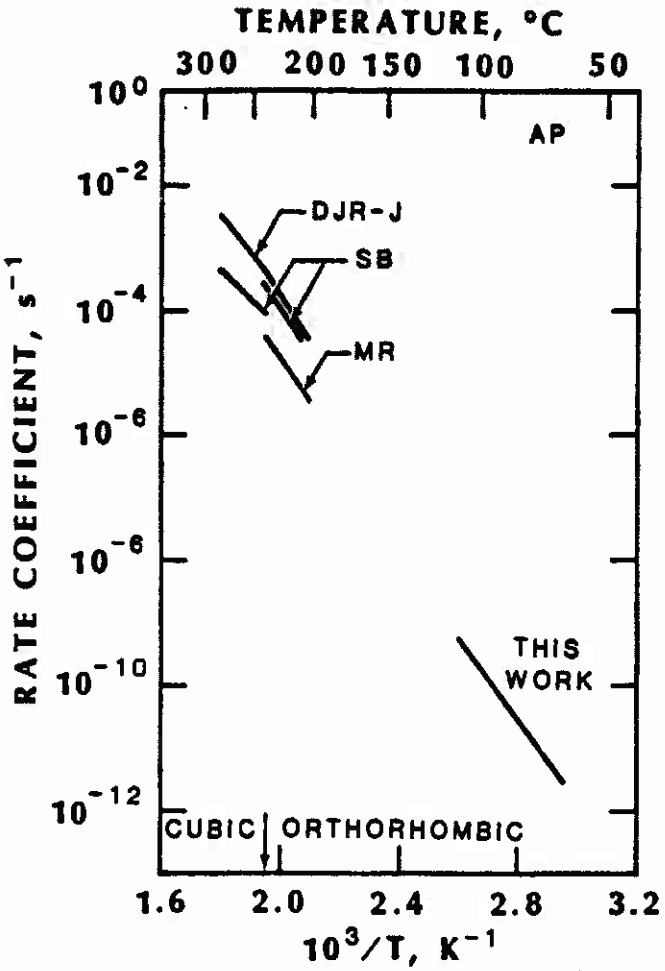

FIGURE 12. COMPARISON OF AP DECOMPOSITION RATE COEFFICIENTS

DJR-J = Ref. 23; SB = Ref. 24; MR = Ref. 25.
The observed activation energies are larger for the orthorhombic solid phase than for the cubic phase.

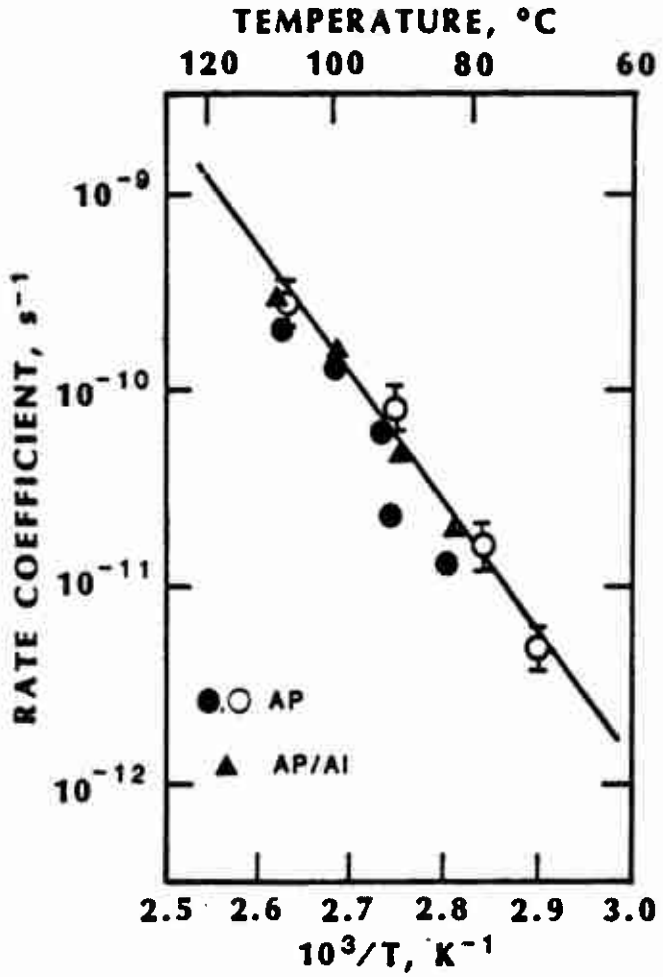

FIGURE 13. ARRHENIUS GRAPH OF AP AND AP/Al DATA

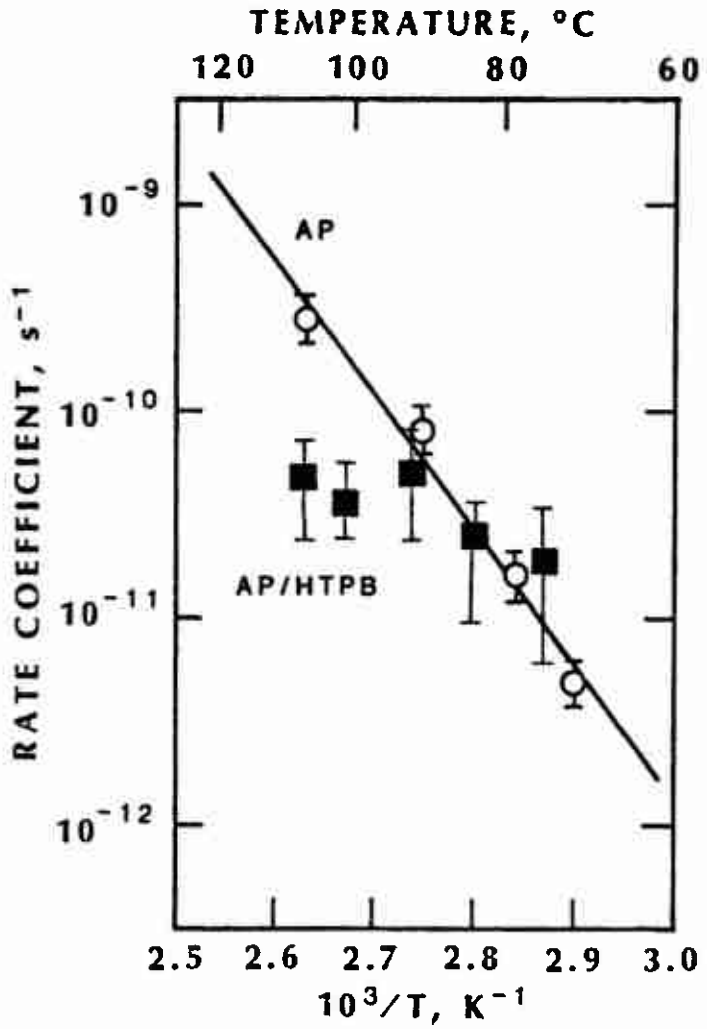

FIGURE 14. ARRHENIUS GRAPH OF AP AND AP/HTPB DATA

TABLE 9

RATE COEFFICIENTS FOR PURE AP AND FOR 50/50 (wt%) AP/Al SAMPLES[a]

Temperature °C	Temperature K	Rate Coefficient, 10^{-10} s^{-1} AP	Rate Coefficient, 10^{-10} s^{-1} AP/Al
83.3	356.5	0.123 ± 0.074	0.190 ± 0.123
91.3	364.5	0.205 ± 0.100	0.483 ± 0.134
99.2	372.4	1.3% ± 0.34	1.70 ± 0.38
107.4	380.6	2.06 ± 0.32	2.83 ± 0.54

[a]Each sample contained 1.20 g of AP. Error bars represent one standard deviation.

diffusion out of the sample. Nevertheless, these data, shown in Fig. 14, indicate that the decomposition products from AP react with the binder, especially at higher temperatures, indicating a significant difference in temperature dependence and hence a large reduction of evolved NH_3 at higher temperatures compared to that from "free" AP. Further experiments would be necessary to quantify this result.

4.1.3 BTTN Decomposition Kinetics

Nitrate esters are used in energetic propellants as plasticizers. In this work, the low temperature stability of the nitrate ester 1,2,4-butanetriol trinitrate, BTTN, was studied. In most propellants containing NG, BTTN, or other nitrate esters, the overall service lifetime of the propellant is determined by the amount of NO_2 produced by decomposition of the relatively unstable nitrate ester and the capacity of the stabilizer in the propellant. BTTN is a viscous, clear, slightly yellow liquid at room temperature with a density of 1.52 g/cm³. It can be loosely considered a tri-nitrate ester substituted n-butane compared to NG which would be tri-nitrate ester substituted propane. Previous studies (Ref. 27) of the decomposition of organic mono- and poly-nitrate esters strongly supports the first step of the decomposition to be fission of the O-NO_2 bond to release NO_2 with activation energies of the order of 160 kJ/mol.

Initial experiments to measure the rate coefficient of BTTN decomposition using the same apparatus as described above for the RDX work were complicated

TABLE 9

RATE COEFFICIENTS FOR PURE AP AND FOR 50/50 (wt%) AP/Al SAMPLES[a]

Temperature °C	Temperature K	Rate Coefficient, 10^{-10} s^{-1} AP	Rate Coefficient, 10^{-10} s^{-1} AP/Al
83.3	356.5	0.123 ± 0.074	0.190 ± 0.123
91.3	364.5	0.205 ± 0.100	0.483 ± 0.134
99.2	372.4	1.3[illegible] ± 0.34	1.70 ± 0.38
107.4	380.6	2.06 ± 0.32	2.83 ± 0.54

[a]Each sample contained 1.20 g of AP. Error bars represent one standard deviation.

diffusion out of the sample. Nevertheless, these data, shown in Fig. 14, indicate that the decomposition products from AP react with the binder, especially at higher temperatures, indicating a significant difference in temperature dependence and hence a large reduction of evolved NH_3 at higher temperatures compared to that from "free" AP. Further experiments would be necessary to quantify this result.

4.1.3 BTTN Decomposition Kinetics

Nitrate esters are used in energetic propellants as plasticizers. In this work, the low temperature stability of the nitrate ester 1,2,4-butanetriol trinitrate, BTTN, was studied. In most propellants containing NG, BTTN, or other nitrate esters, the overall service lifetime of the propellant is determined by the amount of NO_2 produced by decomposition of the relatively unstable nitrate ester and the capacity of the stabilizer in the propellant. BTTN is a viscous, clear, slightly yellow liquid at room temperature with a density of 1.52 g/cm³. It can be loosely considered a tri-nitrate ester substituted n-butane compared to NG which would be tri-nitrate ester substituted propane. Previous studies (Ref. 27) of the decomposition of organic mono- and poly-nitrate esters strongly supports the first step of the decomposition to be fission of the O-NO_2 bond to release NO_2 with activation energies of the order of 160 kJ/mol.

Initial experiments to measure the rate coefficient of BTTN decomposition using the same apparatus as described above for the RDX work were complicated

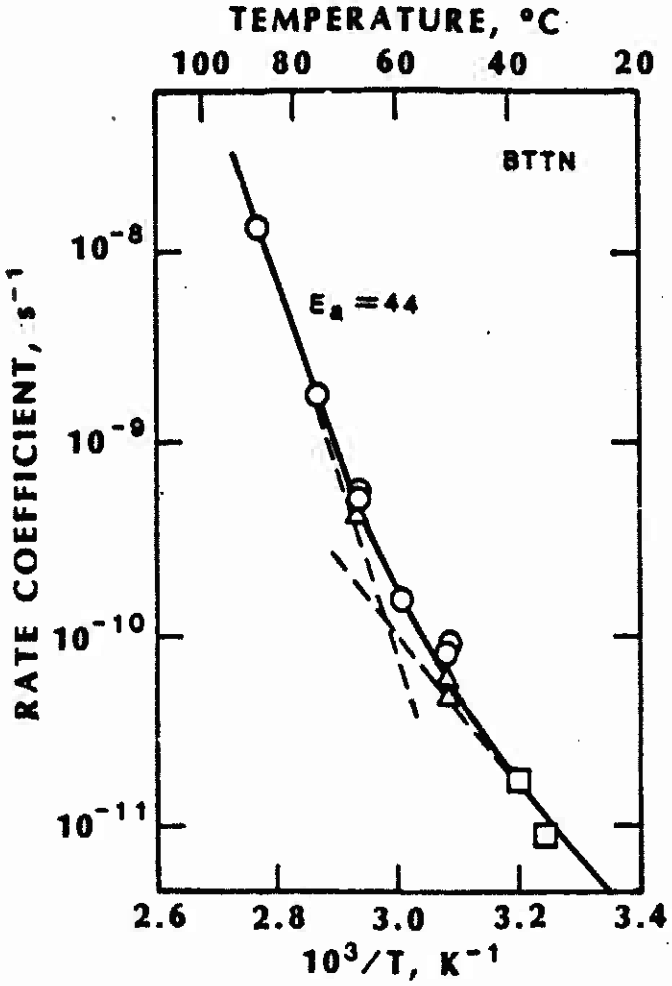

FIGURE 15. ARRHENIUS GRAPH OF BTTN DATA

○ = 0.38 and 0.40 g samples; △ = 0.79 g samples; □ = 1.78 g samples.

than 2 ppb. To obtain data at lower temperatures, a single larger sample of 1.78 g was used which gave the results shown in the figure as squares. The lower activation energy at the lower temperatures is apparent. Finally, experiments were performed using 0.79 g samples to obtain a systematic set of data on the effects of sample size over a common range of temperature (see Table 10). Although the effect was relatively small, the larger samples gave smaller observed decomposition rate coefficients. The curvature shown in Fig. 15 is not, however, caused by a sample size effect; this effect, if of any significance, would reduce the observed curvature.

To investigate the sample size effect quantitatively, another test was performed by flowing the N_2 carrier gas in series through the four sample cells to accumulate a higher concentration of decomposition products. This was done using three 0.40 g samples and one 0.79 g sample. The resulting total NO_x concentration was attributed to the decomposition of a nominal 1.9 g of BTTN. The rate coefficients, given in Table 10, from this experiment at 312, 320, and 332 K were systematically larger than those obtained from the smaller samples by about a factor of two. However, the activation energy computed from these data was about 109 kJ/mol, similar to that for the other data on larger size samples in this temperature range. Two observations can be made from these experiments on sample size. First, with constant sample surface area (0.38-0.40, 0.79, and 1.78 g samples each fill the bottoms of the sample bottles, and so have the same exposed surface area), larger samples give smaller rate coefficients. Second, similar samples with different surface areas (the 1.92 g of BTTN in four cells connected in series has four times the exposed surface area than the single 1.78 g sample) gave rate coefficients that were larger for the sample with the larger exposed area. Thus extrapolating to very small sample size with very large surface area would be expected to give larger rate coefficients on both accounts. All data obtained with various sample sizes or surface areas, however, gave similar slopes in each temperature range.

The data in Fig. 15 cannot be fit to within their statistical uncertainties by a single straight line; thus it appears that the evolved NO_x resulted from the sum of two processes, each rate being first order with a rate coefficient of Arrhenius form. A least squares fit was performed with each data point weighted by the inverse of its uncertainty to determine the four kinetic

parameters. This fit resulted in the following expression, which is represented by the solid line through the data in Fig. 15, for the decomposition of BTTN over the temperature range from 309 to 360 K:

$k = 10^{14.1 \pm 2.0} \exp[-(22400 \pm 1660)/T] + 10^{11.8 \pm 2.1} \exp[-(9060 \pm 2100)/T]\ s^{-1}$.

Thus the higher temperature data exhibit a "normal" (for a nitrate ester) activation energy of 186 ± 14 kJ/mol but a much smaller, 75 ± 18 kJ/mol, value below about 330 K. This rate coefficient expression, extrapolated to 298 K, gives a value of $k = 2.4 \times 10^{-12}\ s^{-1}$, which is about 100 times larger than for RDX and is nearly equal to the decomposition rate coefficient of nitroglycerin.

Thus the following conclusions result from these experiments:

1. Rate coefficients should be given in units which relate sample surface area as well as mass to the observed gas evolution rates.
2. The consistency of the activation energies indicates that the same reaction chemistry is occurring in each case, irrespective of the exposed surface areas.
3. Although the absolute value of the thermal decomposition rate coefficient is of prime importance in specifying the stability of a material at any temperature, the shape of the temperature dependence curve is more important than the absolute value of the rate coefficient in understanding the kinetics of its reaction chemistry. It appears indisputable that two different processes are going on here as was found for NC.

A few measurements of the NO evolution rate coefficient were also made over the temperature range 332 to 360 K. These data, presented in Table 11, demonstrate that about 10% of the NO_x was NO under these conditions and that the activation energy for NO evolution was approximately the same as for NO_2. Analysis of the three higher temperature NO evolution points gives an activation energy of roughly 155 kJ/mol.

The BTTN decomposition rate coefficient obtained in this work is compared in Fig. 16 to data obtained on several other nitrate esters at low temperatures (Refs. 4, 27-29). The data for NG and NIBTN (nitroisobutanetriol trinitrate) are from Phillips, Ref. 27, who discussed the rather large preexponential factors in the Arrhenius rate coefficient expression and the similarity of data obtained for liquid and vapor phase polynitrates. Above

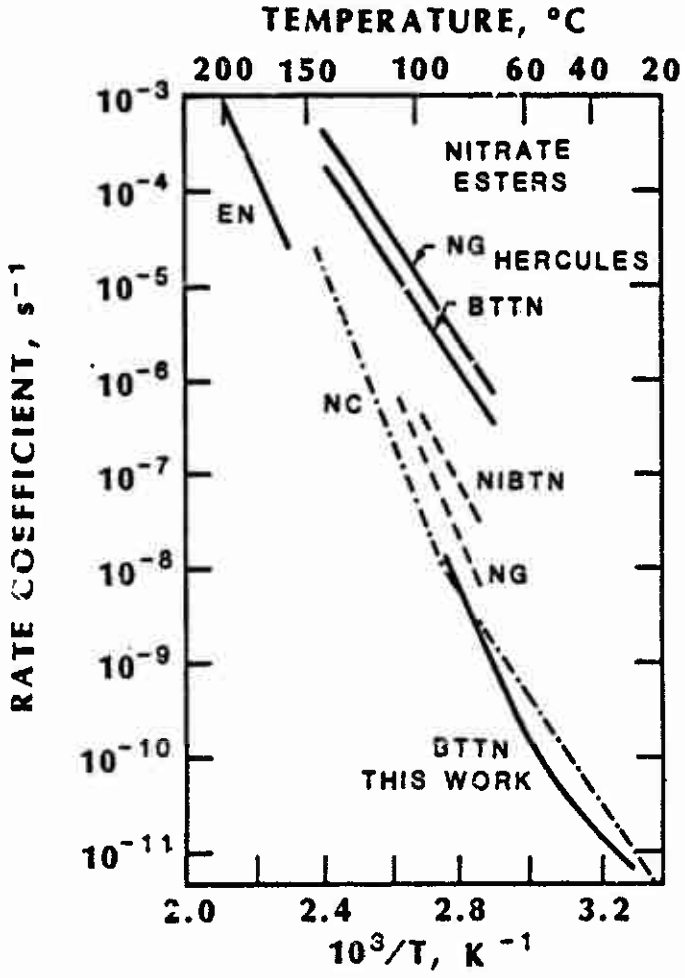

FIGURE 16. COMPARISON OF DECOMPOSITION RATE COEFFICIENTS FOR NITRATE ESTERS

EN = Ethyl nitrate, Ref. 27; NC = Nitrocellulose, Ref. 4;
NIBTN = Nitroisobutanetriol trinitrate, Ref. 27;
NG = Nitroglycerin, Ref. 27; NG, BTTN (Hercules), Ref. 29.

TABLE 11

NO EVOLUTION DATA FOR BTTN

Sample Temperature °C	Sample Temperature K	Rate Coefficients, s^{-1}	Sample Mass, g
87.0	360.2	$(8.6 \pm 1.9) \times 10^{-10}$	0.38[a]
59.1	332.3	$(2.19 \pm 0.71) \times 10^{-11}$	0.40[b]
67.1	340.3	$(4.09 \pm 0.80) \times 10^{-11}$	0.40[b]
75.0	348.2	$(1.67 \pm 0.12) \times 10^{-10}$	0.40[b]

[a]November 1984 data.

[b]December 1984 data.

about 330 K, all of the data show similar slopes except the BTTN and NG data (Ref. 29) labeled "Hercules." These rate coefficients were derived from measurements of the IR absorbance vs. time behavior of dilute mixtures of the nitrate ester in compressed potassium bromide. Five nitrate esters were studied with activation energies obtained over the range 75 to 109 kJ/mol. It has been suggested (Ref. 30) that the disagreement results from the difference in the highly dilute samples in the salt pellets compared with the neat liquid BTTN used in this work; possibly the NO_2 freed in the breaking of a bond is kept in the neighborhood by the liquid long enough for the reverse of the decomposition reaction to occur, thus lowering the observed decomposition rate coefficient. The work of Phillips indicates that this may not be the explanation, but further experiments would be needed to resolve the question.

4.2 PROPELLANT REACTIVITY STUDIES

These tests included (i) "binder reactivity tests," weight gain/loss of binder, sol/gel analysis, and gel permeation chromatography (molecular weight distributions) on mixture samples exposed to reactive gases at 344 K (71°C) for 54 h; and (ii) "chemiluminescence measurements," real time polymer chemiluminescence intensity measurements from samples exposed to reactive gases at several temperatures. All tests were carried out using the propellant mixture series described in Section 3.1, Chemicals and Binder Formulations (Table 1).

4.2.1 Binder Reactivity Tests

The binder reactivity tests were carried out by exposing test discs from each propellant mixture to one of the reactive gases. For each test, four weighed discs were placed in separate thermostated cells which were flushed overnight with N_2 at 313 K (40°C). Then the temperature was increased to 344 K (71°C), the four cells were flushed for about 5 min with either N_2, air, NO, or 5.5% (vol%) NO_2 in air, and then sealed for 54 h. Following this reaction time, the samples were cooled to room temperature, reweighed, sol/gel analyses performed, and GPC analyses performed on the sols. The weight percent sol was calculated by dividing the measured sol mass by the mass of the sample which was organic and multiplying by 100%. The total organic fraction was 100% for samples 1-4, 29% for 5, 30% for 6, and 22% for 7. The sol content for each mixture prior to exposure to reactive gases was also measured and is shown in Table 12 for reference only, since the heating alone in the sample measurement procedure would be expected to alter the binder cure (i.e., change the sol content). Thus we take the data for N_2 after 54 h exposure as

TABLE 12

SOL CONTENT OF UNREACTED PROPELLANT SAMPLES

Sample #	Components	Organic Content, wt%	Sol Content, wt%
1	HTPB/IPDI	100.00	29.9
2	HTPB/IPDI/TPB	100.00	31.2
3	HTPB/IPDI/MNA	100.00	13.0
4	HTPB/IPDI/TPB/MNA	100.00	28.6
5	#4 + AP	28.68	22.0
6	#4 + Al	30.30	27.9
7	#4 + AP/Al	21.88	31.8

the baseline for comparison. The sol contents of the unreacted samples are similar (ca. 30%), except that #3 and #5 appear anomalous. All seven samples were prepared on the same day, cured together, and then refrigerated together

under dry nitrogen. Except for component interactions, these binders should have attained the same degree of curing and sol content. These results indicate that during the initial curing process, differences develop in the degree of binder curing.

The weight percent change and sol content for each sample exposed to the four gas environments are listed in Table 13. (Experiments were terminated on mixture #6 because little effect of adding Al to AP was obtained in the NH_3 evolution experiments.) The results of these tests indicate that each binder adsorbed 1-5 mg of the reactant gas. For the mixtures without stabilizer, the order of adsorption was air * NO) NO_2/air) N_2. The observation that NO gave larger gains than NO_2/air was surprising. However, the ordering of the sol fractions was less systematic as can be seen in Table 13; exposure to NO gave the lowest sol fraction for sample 1 whereas exposure to air produced the lowest sol fraction for sample 2. The weight gain data are shown in Fig. 17 and the sol content data in Fig. 18 for the series of six mixtures exposed to four environments. In Fig. 17, it is apparent that the MNA stabilizer was effective in reducing the weight gain for samples exposed to air (compare samples 1 and 2 without MNA to samples 3 and 4 with MNA, all with no solids). However, upon exposure to NO or to NO_2/air, the MNA stabilizer lost its effectiveness (in terms of weight gain). The addition of AP or AP/Al appear to cause little systematic difference in the observed weight gains. Samples exposed to both nitrogen oxides showed color changes.

The main observation from the sol content data is that sample mixtures with solids were found to be less completely cured. The sol content data shown in Fig. 18 demonstrate the effectiveness of the TPB cure catalyst, showing lower sols for samples 2 and 4 compared with samples 1 and 3 in each case. Thus examining the sample series, 2, 4, 5, and 7 (recall that 6 is not shown), little difference appears between mixtures with and without stabilizer, the addition of AP increases the sol content by roughly 70% (compared to 2 and 4), and addition of AP/Al increases the sol content by a factor of two to three. These observations are without regard to the gas environment to which the samples were exposed. Samples 2 and 4 exposed to air show slightly lower sol contents and, when exposed to NO, slightly higher sol contents than average.

The number and molecular weight distributions, MWD, from the GPC analysis of ARCO R-45M HTPB prepolymer are plotted in Fig. 19. Average MWs were

TABLE 13

SUMMARY OF BINDER REACTIVITY TEST RESULTS[a]

Sample #	Reagent	Weight% Gain	Weight% Sol	Number Average Molecular Wt	Weight Average Molecular Wt
1	Unreacted	----	29.9	10,240	33,120
	N_2	0.17	29.5	9,240	23,590
	Air	1.32	18.5	8,590	22,030
	NO	0.76	15.3	10,750	25,770
	NO_2/Air	0.46	24.5	10,140	24,050
2	Unreacted	----	31.2	8,030	21,100
	N_2	0.28	14.0	6,760	17,550
	Air	0.60	11.0	6,770	17,260
	NO	0.95	15.5	8,000	22,170
	NO_2/Air	0.47	12.9	7,940	21,360
3	Unreacted	----	13.0	8,080	21,890
	N_2	0.07	16.4	7,480	19,610
	Air	0.17	17.2	7,320	19,340
	NO	0.54	19.1	6,850	18,470
	NO_2/Air	0.29	21.6	6,650	17,940
4	Unreacted	----	28.6	8,140	20,840
	N_2	0.03	12.0	6,610	15,450
	Air	0.46	12.4	6,800	17,080
	NO	0.46	16.3	7,840	18,860
	NO_2/Air	0.33	15.0	6,960	16,570
5	Unreacted	----	22.0	9,140	26,620
	N_2	0.02	20.9	7,140	19,360
	Air	0.12	22.4	6,860	18,360
	NO	0.37	26.6	7,430	20,290
	NO_2/Air	0.37	23.9	7,490	20,040
7	Unreacted	----	31.8	9,790	27,210
	N_2	0.07	45.5	7,040	17,960
	Air	0.08	33.7	6,800	18,220
	NO	0.68	37.2	7,230	18,820
	NO_2/Air	0.32	35.2	6,940	19,310

[a]Results after exposure to indicated environment for 54 h at 344 K.

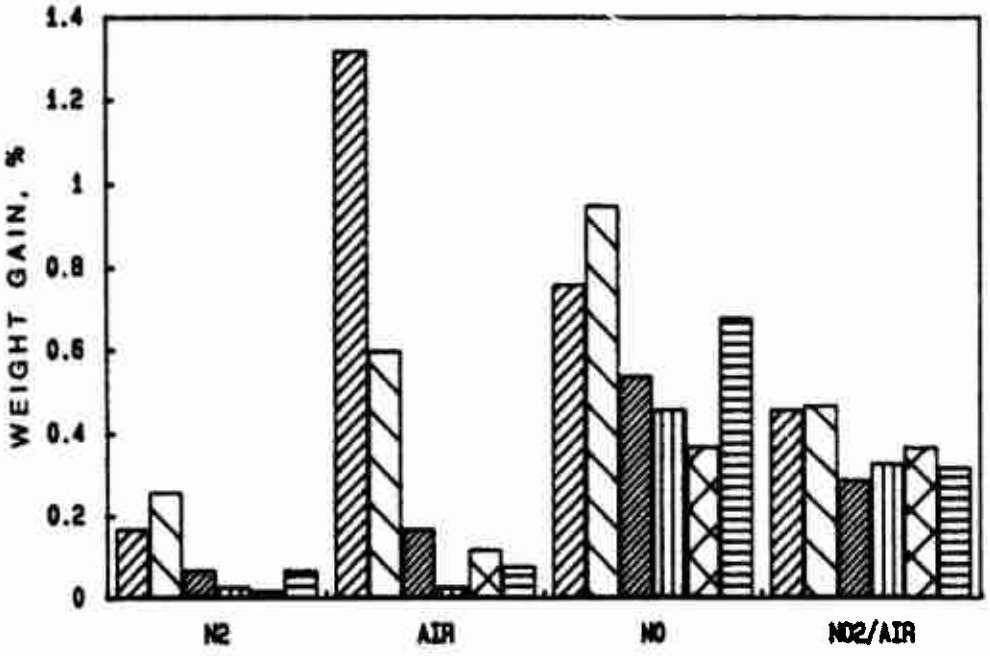

FIGURE 17. WEIGHT GAIN DATA FOR SAMPLES 1-5 AND 7

Exposure for 54 h at 344 K.
The bars represent results for samples 1-5 and 7 in each atmosphere.

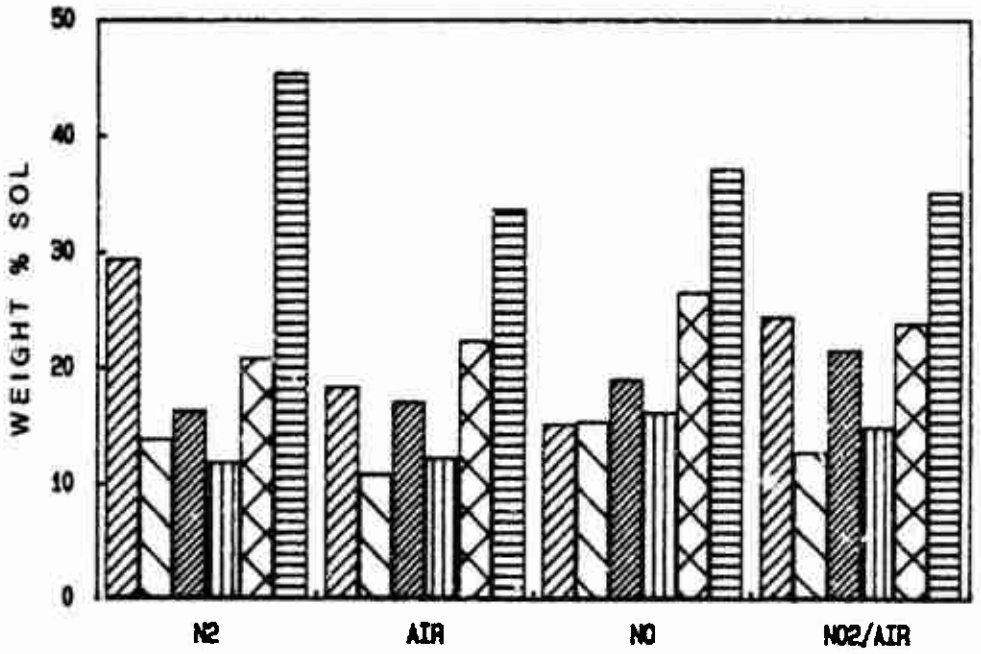

FIGURE 18. SOL PERCENT DATA FOR SAMPLES 1-5 AND 7

Exposure for 54 h at 344 K.
The bars represent results for samples 1-5 and 7 in each atmosphere.

calculated to be 3,160 (number average) and 7,410 (weight average). Figures 20-25 show GPC data for the sols extracted from the six propellant samples exposed to reactive gas environments. The axes scales are identical in Figs. 20-25 for ease of comparison. The number and weight average MWs for the propellant samples are listed in Table 13. THF solvent impurities (we use reagent grade THF, additionally purified by passage through a column of alumina, ferrous ammonium sulfate, and silica gel) observed in the low MW region vary in amount from sample to sample. The region less than 300 Daltons could not be reliably analyzed and the region between 300 and 1000 Daltons was considered to be an unreliable measure of the binder characteristics. These data were therefore not plotted on Figs. 20-25, but average MWs were calculated using 100 and 500 Daltons as lower cutoff points for the analysis of the GPC traces in addition to the standard 1000 Dalton lower cutoff (Table 13). These alternate number and weight averaged MWs are listed in Table 14 but are not further considered in this report.

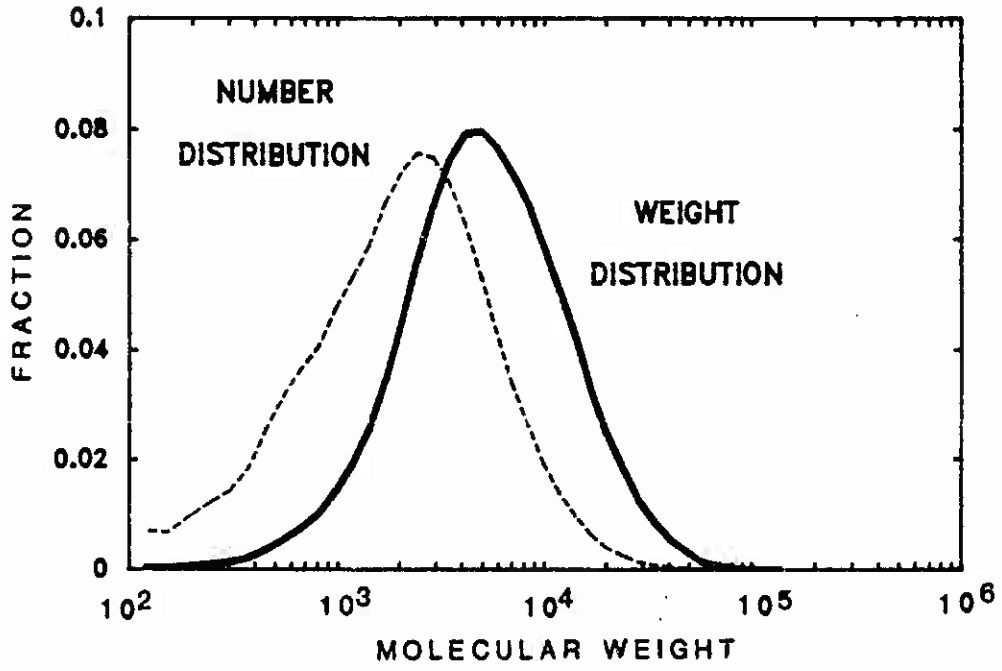

FIGURE 19. MOLECULAR WEIGHT DISTRIBUTION OF HTPB PREPOLYMER

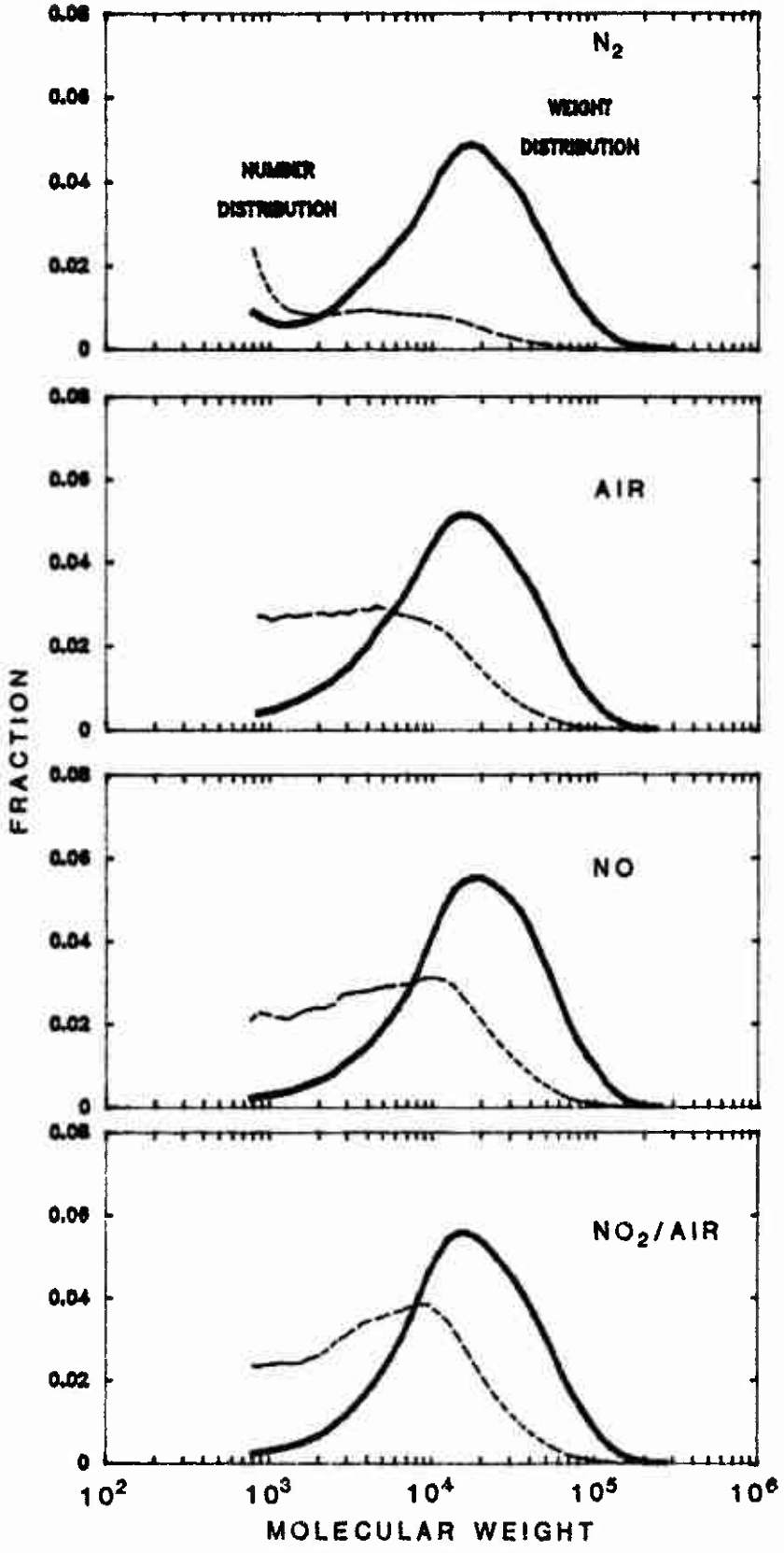

FIGURE 20. SOL PERCENT DATA FOR SAMPLE 1

Exposure for 54 h at 344 K in indicated atmospheres.

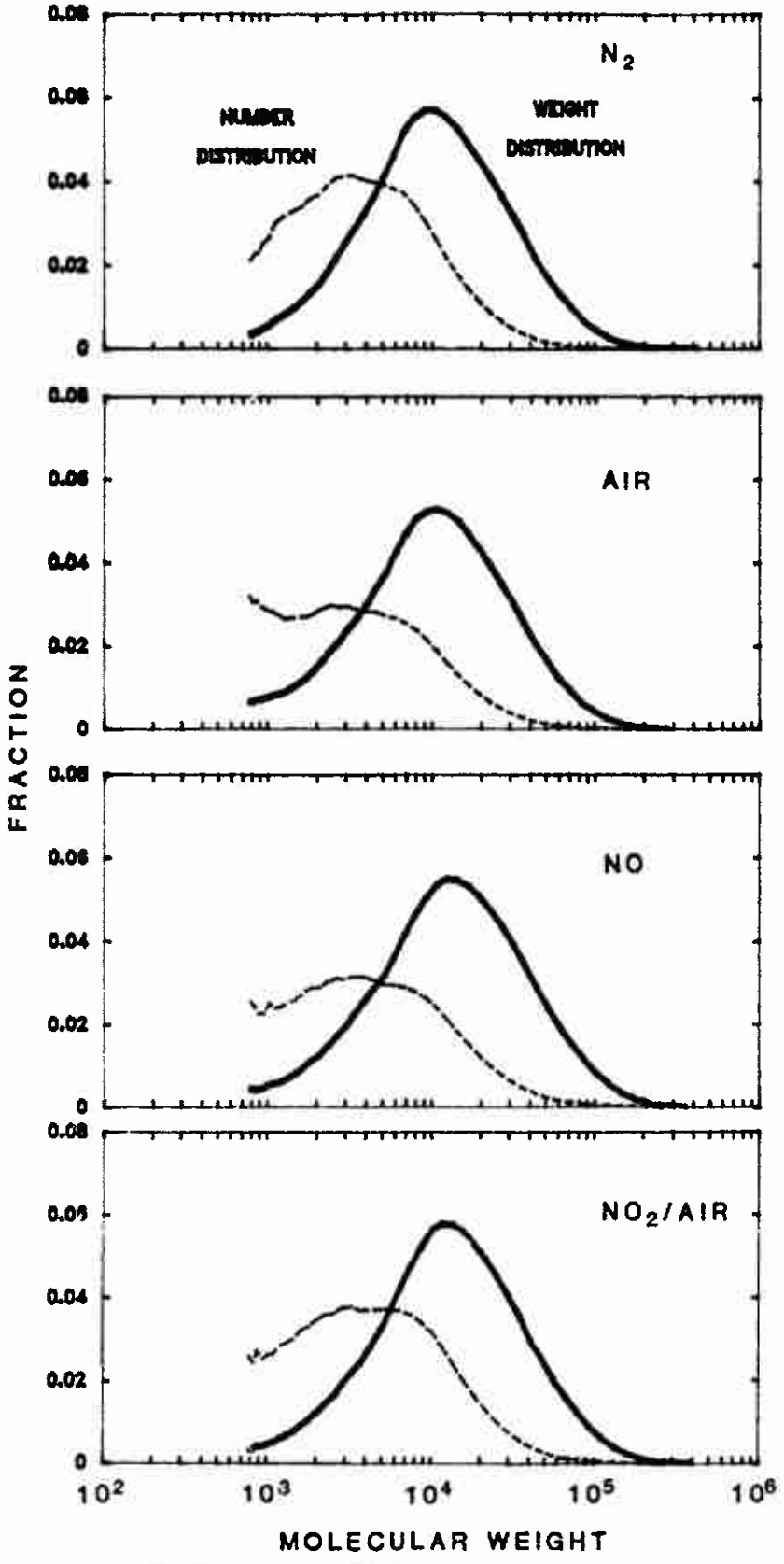

FIGURE 21. SOL PERCENT DATA FOR SAMPLE 2

Exposure for 54 h at 344 K in indicated atmospheres.

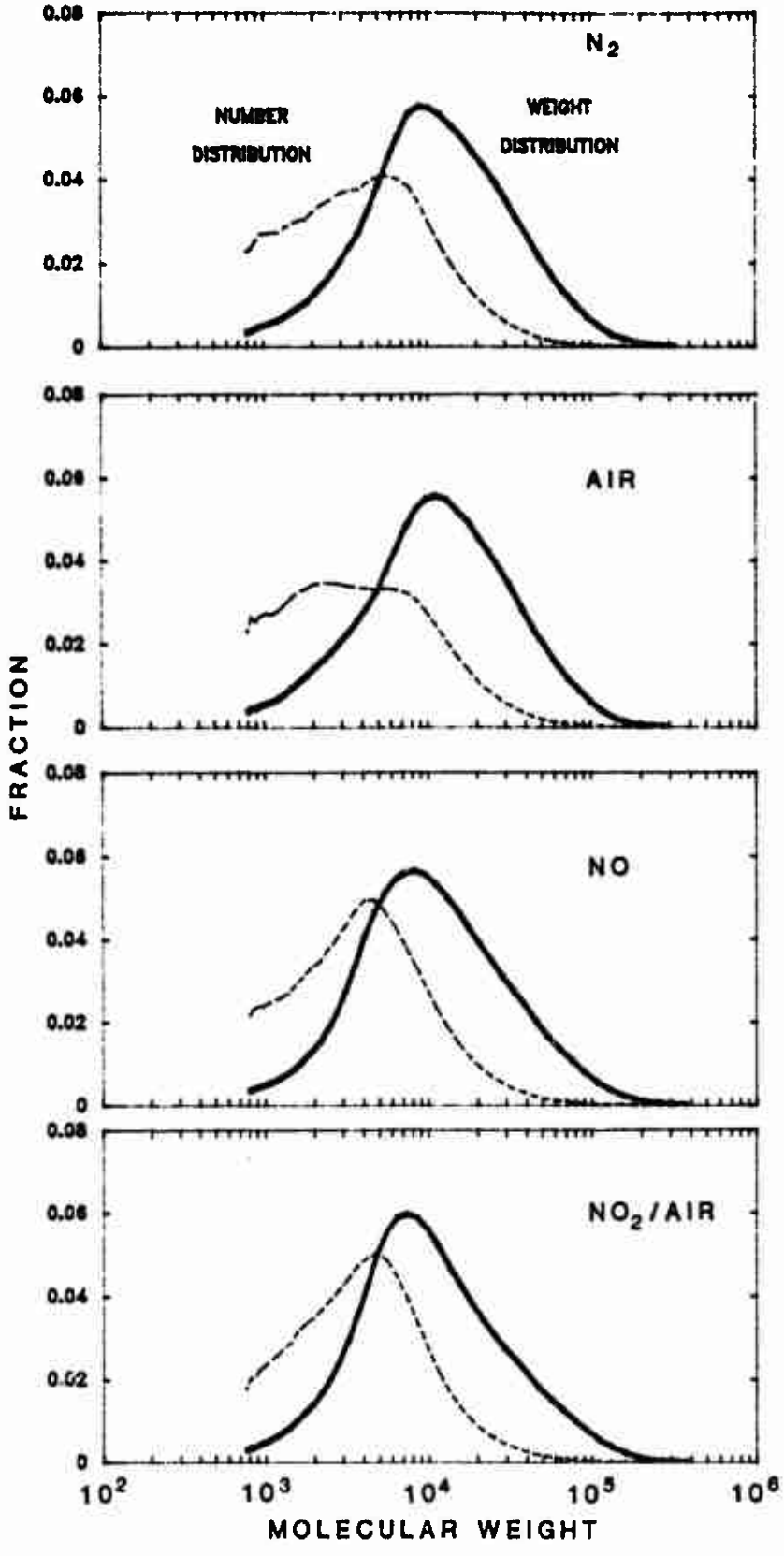

FIGURE 22. SOL PERCENT DATA FOR SAMPLE 3

Exposure for 54 h at 344 K in indicated atmospheres.

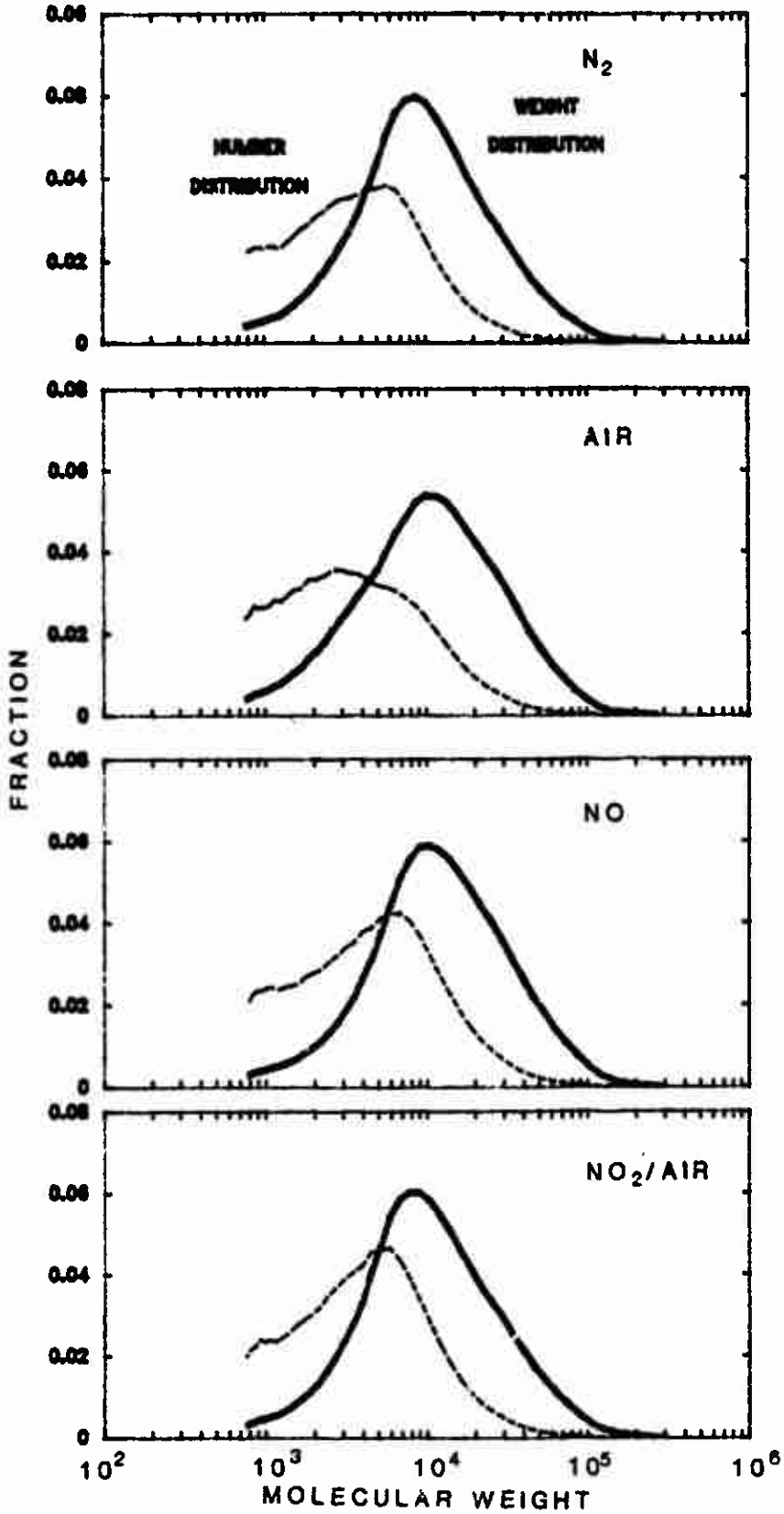

FIGURE 23. SOL PERCENT DATA FOR SAMPLE 4

Exposure for 54 h at 344 K in indicated atmospheres.

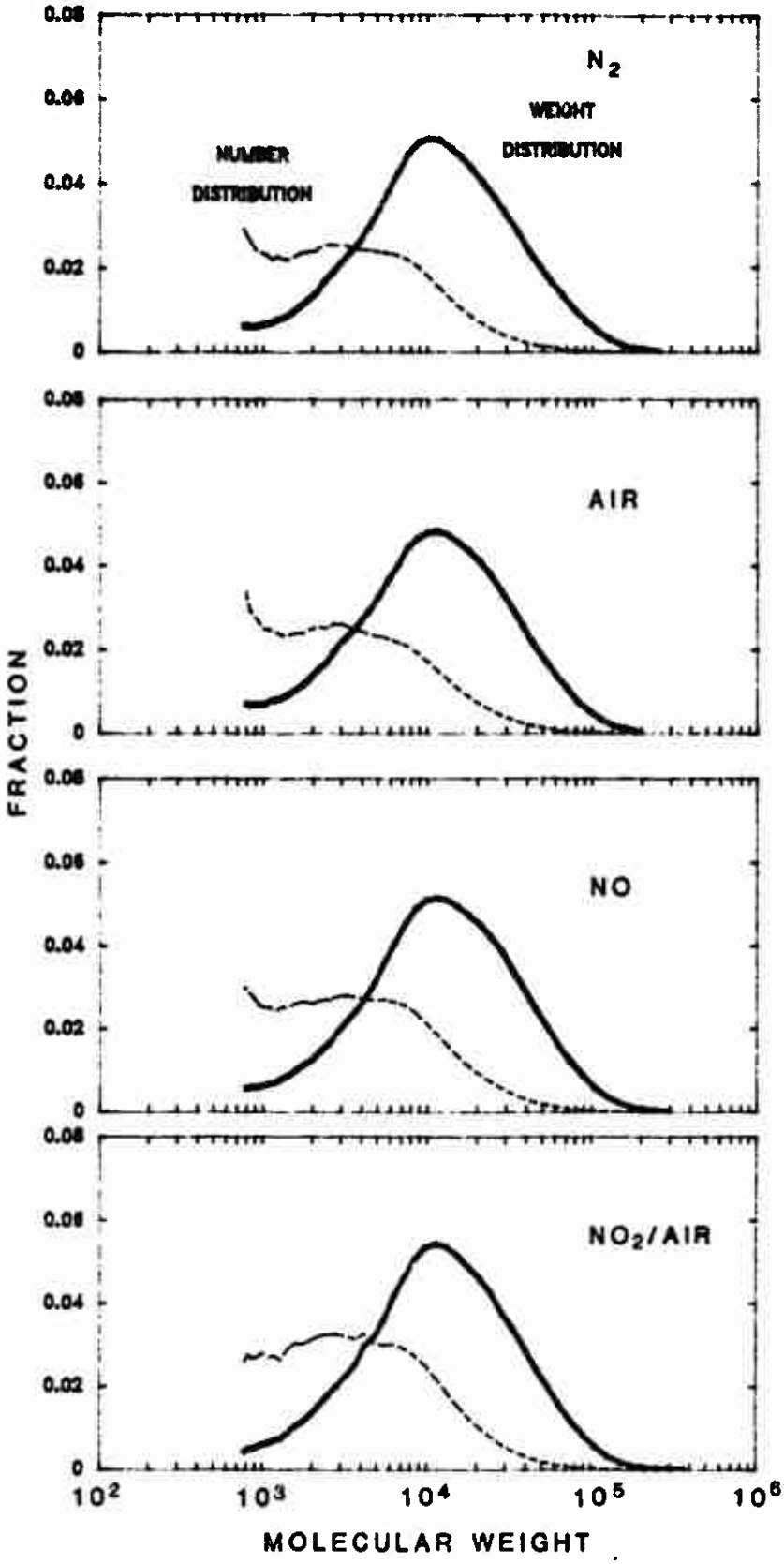

FIGURE 24. SOL PERCENT DATA FOR SAMPLE 5

Exposure for 54 h at 344 K in indicated atmospheres.

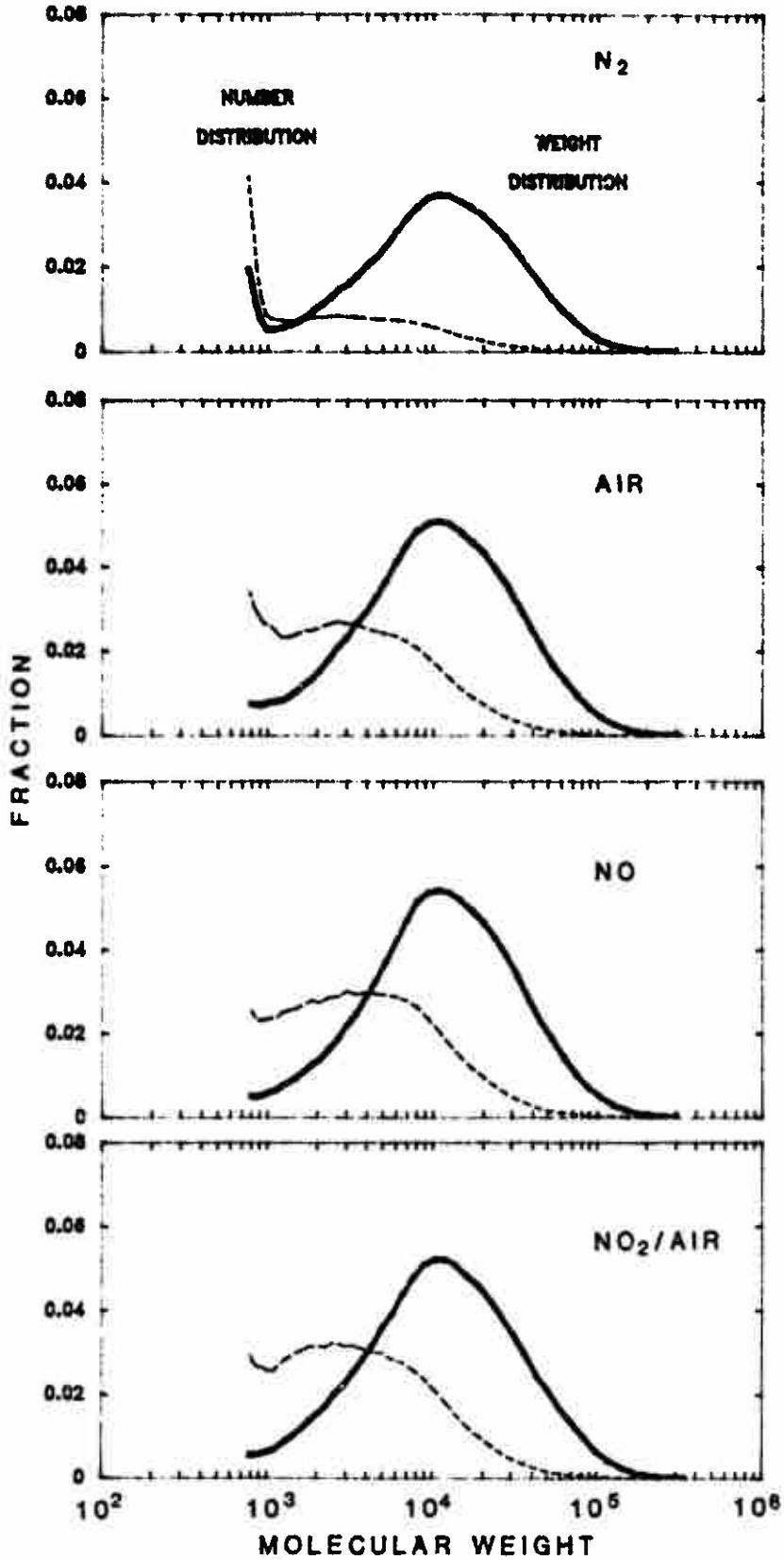

FIGURE 25. SOL PERCENT DATA FOR SAMPLE 7

Exposure for 54 h at 344 K in indicated atmospheres.

TABLE 14

ALTERNATE ANALYSIS OF GPC DATA USING DIFFERENT LOWER MW CUTOFFS

Sample #	Reagent	Number Average Molecular Wt (≥100 Daltons)	Weight Average Molecular Wt (≥100 Daltons)	Number Average Molecular Wt (≥500 Daltons)	Weight Average Molecular Wt (≥500 Daltons)
1	Unreacted	2,920	30,050	7,960	32,320
	N_2	2,790	20,540	5,390	22,180
	Air	6,330	21,420	7,110	21,590
	NO	8,260	25,300	9,140	25,430
	NO_2/Air	8,440	23,690	8,820	23,740
2	Unreacted	2,840	19,040	6,340	20,540
	N_2	6,120	17,310	6,150	17,320
	Air	5,430	16,710	5,540	16,750
	NO	6,770	21,780	6,880	21,780
	NO_2/Air	7,180	21,110	7,200	21,120
3	Unreacted	5,480	21,250	6,970	21,530
	N_2	6,700	19,340	6,730	19,350
	Air	6,450	19,030	6,500	19,040
	NO	6,170	18,210	6,200	18,220
	NO_2/Air	6,000	17,670	6,040	17,680
4	Unreacted	5,290	20,070	6,820	20,470
	N_2	5,720	15,130	5,800	15,160
	Air	5,880	16,730	7,140	16,750
	NO	7,100	18,640	7,140	18,650
	NO_2/Air	6,250	16,320	6,280	16,330
5	Unreacted	2,140	22,940	7,370	26,070
	N_2	5,520	18,710	5,680	18,770
	Air	5,400	17,770	5,520	17,810
	NO	6,080	19,780	6,180	19,820
	NO_2/Air	6,280	19,590	6,360	19,610
6	Unreacted	2,300	24,870	8,460	28,330
	N_2	-----	------	-----	------
	Air	-----	------	-----	------
	NO	-----	------	-----	------
	NO_2/Air	-----	------	-----	------
7	Unreacted	2,580	23,320	5,440	25,540
	N_2	3,200	15,720	3,750	16,240
	Air	5,230	17,560	5,410	17,640
	NO	5,970	18,370	6,090	18,400
	NO_2/Air	5,820	18,860	5,920	18,900

The molecular weight distributions, MWDs, can be overlaid and analyzed for differences due to the exposure to different gas environments. An example of this is shown in Fig. 26 for weight MWD of sample 4 exposed to the four environments. The differences are seen to be rather small, with changes in the curve shapes possibly being more important than the positions of their maxima. The number and weight averaged MWs are defined to include information on, for example, the skewness of this type of curves and these data are plotted in Figs. 27 and 28. Interpretation of these data was found to be difficult. The analysis of sample 1 may be an anomaly; possibly it was not completely cured, thus giving the higher molecular weights compared with the other samples.

The main observations from the sol/gel analyses therefore were that the TPB cure catalyst noticeably decreases the sol fraction and that the samples with added solids give significantly larger sol fractions. Surprisingly, no real differences in sol fraction were found among samples exposed to the different gas environments. The GPC analyses of the polymer molecular weight distributions in these sol fractions also showed only minor differences. Exposure to NO yielded a slightly larger MW for most samples. No significant differences were seen between the samples with and without solids. This

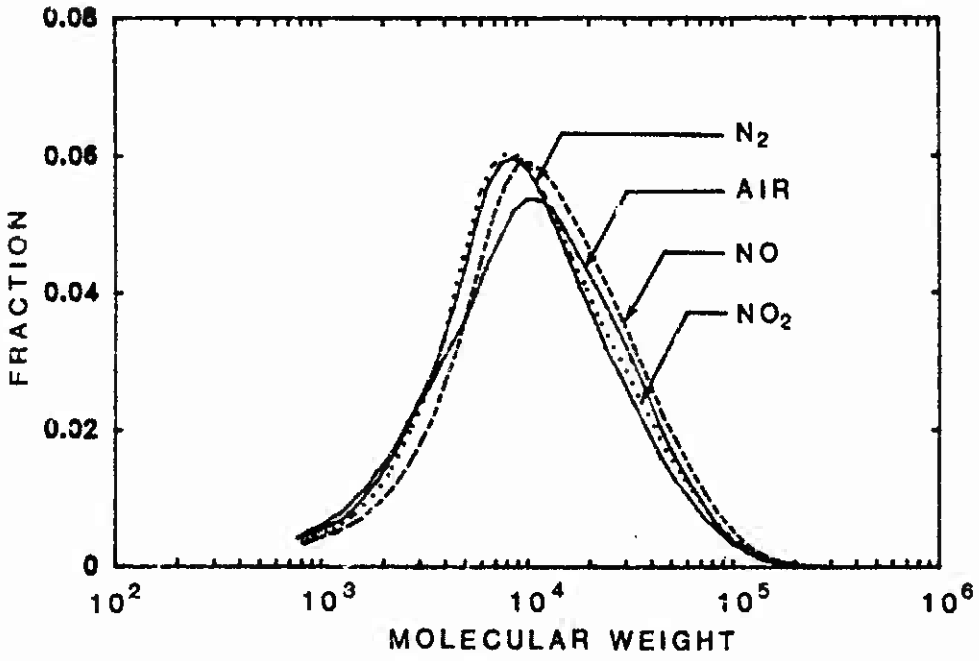

FIGURE 26. MOLECULAR WEIGHT DISTRIBUTIONS FOR SAMPLE 4

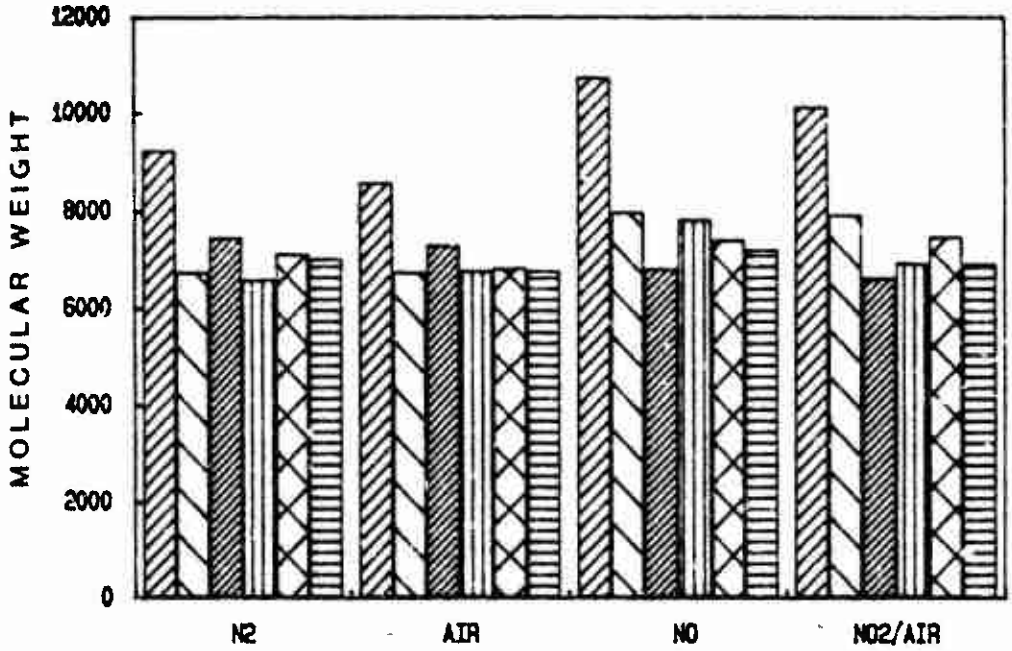

FIGURE 27. WEIGHT AVERAGED MOLECULAR WEIGHTS FOR SAMPLES 1-5 AND 7

The bars represent results for samples 1-5 and 7 in each atmosphere.

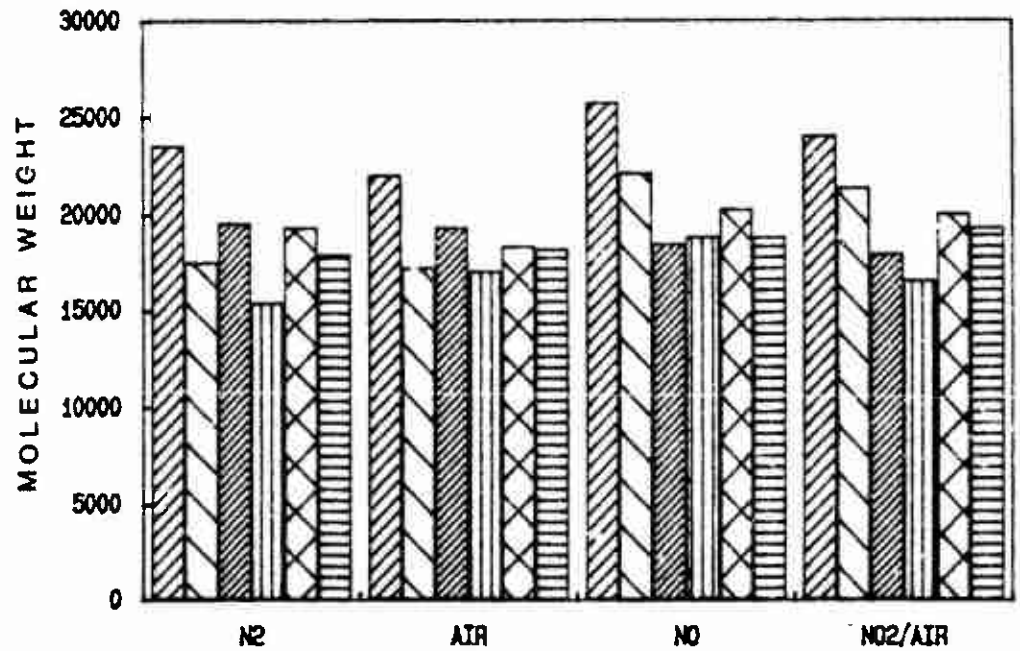

FIGURE 28. NUMBER AVERAGED MOLECULAR WEIGHTS FOR SAMPLES 1-5 AND 7

The bars represent results for samples 1-5 and 7 in each atmosphere.

indicates that AP addition, and even more so, AP and Al addition, greatly increased the sol weight fraction without changing the MW of the polymer that is in the sol. This probably means that the cure reactions were hindered by the solids.

In general, the results obtained in this work indicate that sol/gel fraction analysis and molecular weight analysis by GPC are not sufficiently sensitive or are not sensitive to the right factors to easily and reliably show small changes in this type of propellant.

4.2.2 Chemiluminescence Measurements

An example of the raw data as recorded by the MCS after background subtraction is shown in Fig. 29. Polymer CL data were obtained on samples 1-4 for the four reagents at four temperatures. In our initial work,

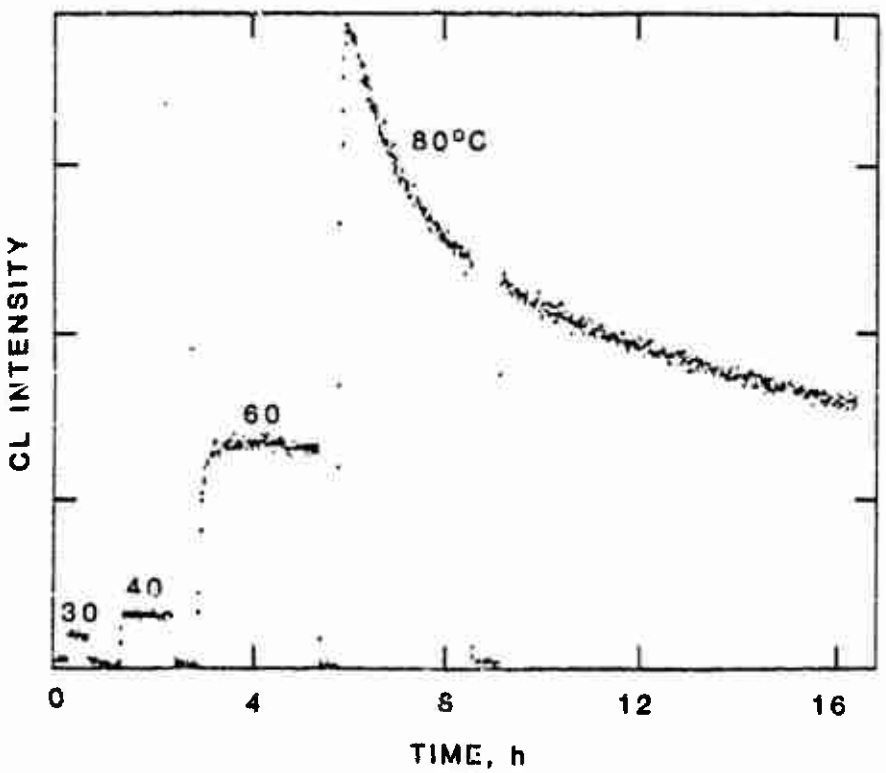

FIGURE 29. CHEMILUMINESCENCE FROM SAMPLE 2 EXPOSED TO AIR

Background and dark signals between the chemiluminescence at each temperature.

both short term CL intensities, often exhibiting a peak, and final steady state intensity values were obtained. The steady state values required a long time to obtain, sometimes greater than 24 h, at the highest temperatures. We therefore correlated the peak intensity values with the steady state intensity values and concluded that no additional information was being obtained from the long term data. Only peak (i.e., short term) CL intensities are therefore reported and analyzed. The results of weighted least squares fits to these data are given in Table 15. Generally the results from the four gas environments divide into two groups; data for air and NO_2/air in one group and for N_2 and NO/N_2 in the other. Activation energies are in the range of about 38-54 kJ/mol. Since all of these slope parameters are similar, considering their

TABLE 15

SUMMARY OF PROPELLANT CL TEST RESULTS[a]

Sample #	Reagent	"a" Factor min^{-1}	Activation Energy kJ/mol	Peak CL at 323 K[b] min^{-1}
1	N_2	10.82 ± 0.47	51.76 ± 3.14	279
	Air	10.74 ± 0.26	43.85 ± 1.71	2262
	NO/N_2	8.81 ± 0.60	40.33 ± 3.97	196
	NO_2/Air	11.80 ± 0.66	52.41 ± 4.19	2166
2	N_2	9.35 ± 1.09	44.15 ± 7.29	169
	Air	11.77 ± 0.85	51.67 ± 5.41	2854
	NO/N_2	9.70 ± 0.30	46.36 ± 1.98	158
	NO_2/Air	11.04 ± 0.40	48.02 ± 2.57	1899
3	N_2	11.03 ± 0.80	54.66 ± 5.32	156
	Air	11.05 ± 0.81	48.39 ± 5.28	1678
	NO/N_2	10.51 ± 0.29	50.95 ± 1.95	188
	NO_2/Air	9.51 ± 0.80	36.11 ± 5.16	4709
4	N_2	9.62 ± 0.13	49.54 ± 0.87	40
	Air	11.73 ± 0.43	52.39 ± 2.81	1808
	NO/N_2	8.02 ± 2.06	37.91 ±13.54	77
	NO_2/Air	8.17 ± 0.43	27.41 ± 2.81	5543

[a]Peak CL data fit to (counts/min) = 10^a exp(-Ea/RT). Uncertainties are ± one standard deviation.

[b]Values calculated from fitting equation.

uncertainties, a possibly more meaningful comparison of the CL intensity (photon count per minute) at 323 K (50°C) obtained from the averaged fits to both sets of data for each sample is included in Table 15. The consistent large difference between all samples exposed to N_2 or NO/N_2 and those exposed to air or NO_2/air is seen. There seems to be no difference between results for sample 1 and sample 2, indicating that the mixtures were probably fully cured (by 10 days at 330 K and 24 h at 359 K) and that the addition of TPB caused no effect. For the samples exposed to air, the effect of the MNA stabilizer is demonstrated by the ≈ 50% reduction in the CL intensity for samples 3 and 4 compared to samples 1 and 2. However, it is notable that the MNA addition apparently did not similarly stabilize the sample exposed to NO_2/air, since samples 3 and 4 have CL intensities larger than for samples 1 and 2.

All of the CL data exhibited Arrhenius behavior, that is, yielded a straight line when the logarithm of the CL intensity (photon count rate) was plotted vs. inverse temperature. In each case, the data obtained from samples exposed to N_2 and to NO were similar and were about a factor of 15 smaller than the data obtained from samples exposed to air or NO_2/air. The activation energies were almost all found to be about 40 to 50 kJ/mol with typical standard deviations of about ± 4 kJ/mol. The differences in activation energies with different sample compositions and upon exposure to different gas environments were not found to be significant. One point of note was that the presence of the MNA stabilizer was found to significantly reduce the CL upon exposure to air, but not upon exposure to NO_2/air. It was found that the NO environment did not produce the CL from the polymer. This is reasonable since the conventional reaction mechanism (Refs. 6, 7) for HTPB oxidation involves a radical chain reaction. NO has long been used as a radical scavenger in conventional kinetic studies, and if it interrupted the above reaction sequence, the CL, which is generally proposed to be produced from peroxide recombination, would be reduced. The radical propagation chain also requires the presence of O_2. Thus the oxidation of the binder would be expected to be less upon exposure to NO than upon exposure to air or NO_2/air. The binder reactivity results, discussed above, however, show more or at least as much weight gain and sol fraction for exposure to NO as for air. The GPC analyses of the binder sols show slightly higher averaged molecular weight values for NO exposure than for air or NO_2/air exposure.

The results of this program demonstrate the ability of the real time chemiluminescence NO_x offgas analysis technique to measure low temperature kinetic parameters important to understanding propellant service lifetimes and the initial stages of propellant combustion. The studies of increasingly complex HTPB-containing mixtures by standard analysis techniques and by a novel solid state chemiluminescence technique contribute important data to help decipher HTPB-containing solid propellant aging chemistry. Additional experimental work (for example, IR spectra of propellants before and after exposure to reactant gases) is needed using highly sensitive techniques to study binder degradation and further analytical work to understand these and other results and to expand the understanding of the reaction chemistry to other propellant binders.

5. REFERENCES

1. Vassil'ev, R. F., "Chemiluminescence in Liquid Phase Reactions." Progress in Reaction Kinetics, Vol. 4, pp. 305-352, 1967.

2. Davenport, J.E. and Mayo, F.R., Chemiluminescence for Aging," AFRPL TR-85-072, SRI International, Menlo Park, CA, November 1985.

3. Fifer, R. A., "Chemistry of Nitrate Ester and Nitramine Propellants," in Fundamentals of Solid-Propellant Combustion, K.K. Kuo, and M. Summerfield, Eds., American Institute of Aeronautics and Astronautics, New York, NY, 1984, Chap. 4.

4. Volltrauer, H.N. and Fontijn, A., "Low Temperature Pyrolysis Studies by Chemiluminescence Techniques. Real-Time Nitrocellulose and PBX 9404 Decomposition." Combustion and Flame, Vol. 41, pp. 313-324, 1981.

5. Layton, L. H., Jones, L. L., and Raisor, R. C., Chemi-Structural Aging of Minimum Smoke Propellants, AFRPL TR-82-062, Thiokol Corp., Brigham City, UT, December 1982.

6. Dunn, J. R., "Aging and Degradation." in The Stereo Rubbers, W. M. Saltman, Ed., Wiley, New York, NY, 1977, Chap. 9.

7. McNeill, I. C. and Stevenson, W. T. K., "The Structure and Stability of Oxidized Polybutadiene." Polymer Degradation and Stability, Vol. 11, pp. 123-143, 1985.

8. Standard Test Method for Molecular Weight Distribution of Certain Polymers by Liquid Exclusion Chromatography (Gel Permeation Chromatography - GPC) Using Universal Calibration, ASTM/ANSI D 3593-77, American Society for Testing and Materials, Philadelphia, PA, 1977.

9. Standard Test Method for Molecular Weight Averages and Molecular Weight Distribution of Polystyrene by Liquid Exclusion Chromatography (Gel Permeation Chromatography - GPC), ASTM/ANSI D 3536-76, American Society for Testing and Materials, Philadelphia, PA, 1976.

10. Handbook of Physics and Chemistry, 65th Ed., CRC Press, Boca Raton, FL, 1984-1985, p. F-157.

11. Law, R., Personal communication concerning HTPB standard, Morton Thiokol, Inc., Wasatch Division, Brigham City, UT, 18 October 1985.

12. Schroeder, M.A., Critical Analysis of Nitramine Decomposition Data: Activation Energies and Frequency Factors for HMX and RDX Decomposition, a) Seventeenth JANNAF Combustion Meeting, CPIA Publ. 329, Vol. II, pp. 493-508, November 1980; b) Sixteenth JANNAF Combustion Meeting, CPIA Publ. 308. Vol. II, pp. 17-34, December 1979.

13. McCarty, K.P., HMX Propellant Combustion Studies, a) AFRPL-TR-79-61, November 1979; b) AFRPL-TR-78-73, November 1978; c) AFRPL-TR-76-59, December 1976, Air Force Rocket Propulsion Laboratory, Edwards Air Force Base, CA.

14. Batten, J.J. and Murdie, D.C., "Decomposition of RDX at Temperatures Below the Melting Point." Australian Journal of Chemistry a) Vol. 23, pp. 737-747, 1970; b) Vol. 23, pp. 749-755, 1970; c) Vol. 24, pp. 945-954, 1971; d) Vol. 24, pp. 2025-2029, 1971; e) Vol. 25, pp. 2337-2351, 1972.

15. Cosgrove, J.D. and Owen, A.J., "The Thermal Decomposition of 1,3,5-Trinitrohexahydro-1,3,5-triazine (RDX)." a) Combustion and Flame Vol. 22, pp. 13-18, 1974; b) Vol. 22, pp. 19-22, 1974.

16. Rauch, F.C. and Fanelli, A.J., "The Thermal Decomposition Kinetics of Hexadydro-1,3,5-trinitro-s-triazine above the Melting Point: Evidence for Both Gas and Liquid Phase Decomposition." Journal of Physical Chemistry, Vol 73, No. 5, pp. 1604-1608, May 1969.

17. Oyumi, Y. and Brill, T. B., "Thermal Decomposition of Energetic Materials 3. A High-Rate, In Situ, FTIR Study of the Thermolysis of RDX and HMX with Pressure and Heating Rates as Variables," Combustion and Flame, Vol. 62, No. 3, pp. 213-224, December 1985.

18. Oyumi, Y. and Brill, T. B., "Thermal Decomposition of Energetic Materials 9. A Relationship of Molecular Structure and Vibrations to Decomposition: Polynitro-3,3,7,7-tetrakis(trifluoromethyl)-2,4,6,8-tetraazabicyclo [3.3.0]octanes." Journal of Physical Chemistry Vol. 90, pp. 2679-2682, 1986.

19. Brunauer, S., Emmett, P. H., and Teller, E., "Adsorption of Gases in Multimolecular Layers." Journal of the American Chemical Society, Vol. 60, pp. 309-319, 1938.

20. Cundall, R.B., Palmer, T.F., and Wood, C.E.C., "Vapor Pressure Measurements on Some Organic High Explosives." Journal of the Chemical Society, Faraday Transactions I, Vol. 74, pp. 1339-1345, 1978.

21. Rogers, R. N. and Daub, G. W., "Scanning Calorimetric Determination of Vapor-Phase Kinetic Data." Analytical Chemistry, Vol. 45, No. 3, pp. 596-600, March 1973.

22. Shaw, R. and Walker, F.E., "Estimated Kinetics and Thermochemistry of Some Initial Unimolecular Reactions in the Thermal Decomposition of 1,3,5,7-Tetranitro-1,3,5,7-tetraazacyclooctane in the Gas Phase." Journal of Chemical Physics, Vol. 81, No. 25, pp. 2572-2576, November 1977.

23. Davies, J. V., Jacobs, P. W. V., and Russell-Jones, A., "Thermal Decomposition of Ammonium Perchlorate." Transactions of the Faraday Society Vol. 63, No. 535, pp. 1737-1748, July 1967.

24. Solymosi, F. and Borcsok, S., "Decomposition and Ignition of Ammonium Perchlorate in a Stream of Perchloric Acid Vapor," Sixteenth Symposium (International) on Combustion, The Combustion Institute, Pittsburgh, Pa 1976, pp. 1235-1241.

25. Manelis, G. B. and Rubtsov, Yu. I., Zhurnal Fiziki Khimi, Vol. 40, pp. 770, 1966.

26. Jacobs, P. W. M. and Whitehead, H. M., "Decomposition and Combustion of Ammonium Perchlorate." Chemical Reviews, Vol. 69, pp. 551-590, 1969.

27. Phillips, L., "Thermal Decomposition of Organic Nitrates." Nature, Vol. 160, pp. 753-754, 1947.

28. Levy, J. B., "The Thermal Decomposition of Nitrate Esters. I. Ethyl Nitrate." Journal of the American Chemical Society, Vol. 76, pp. 3254-3257, 1954.

29. Rodeheaver, O. G., Elrick, O. E., and Ebeling, C. E., Naval Sea Systems Command Research and Exploratory Development - 1975, OCN-N-54-6 (A04057-101-07-010), Hercules Inc./Allegany Ballistics Laboratory, February 1976.

30. Goshgarian, B.B., Personal communication concerning nitrate ester decompositions, Project Officer, Air Force Rocket Propulsion Laboratory, Edwards Air Force Base, CA, October 1984.

APPENDIX A

HTPB LOT ANALYSIS SUPPLIED BY ARCO

Customer: Mr. Robert Gill
AeroChem Research Labs.

Reference: Your request 6/10/85

Location: P.O. Box 12
Princeton, NJ 08542

Lot No.: 303065

PROPERTY	ANALYSIS
Nonvolatile Material, wt%	99.9
Hydroxyl Value, meq/g	0.71
Viscosity, Ps @ 30°C	44
Water Content, wt%	0.03
Unsaturation Type, wt%	
Trans, 1-4	53.5
Cis, 1-4	19.5
Vinyl, 1-2	27.0
Total Peroxides, as H_2O_2, ppm	230
CCl_4 Insolubles, wt%	0.08
Sulfated Ash, wt%	< 0.01
Iodine Number	438
Specific Gravity	0.9005
APHA Color	10

Ms. Kay Gormley
June 10, 1985